MICE HARBORING A *Pnkd* NONSENSE MUTATION ASSOCIATED WITH TOURETTE DISORDER HAVE BEHAVIORAL ABNORMALITIES DISTINCT FROM THOSE OBSERVED IN *Pnkd* KNOCKOUT MICE

By

CARA MARIE NASELLO

School of Graduate Studies

Rutgers, The State University of New Jersey

In partial fulfillment of the requirements

For the degree of

Doctor of Philosophy

Graduate Program in Microbiology and Molecular Genetics

Written under the direction of

Jay Tischfield

And approved by

_____

_____

_____

_____

New Brunswick, New Jersey

January 2018

ABSTRACT OF THE DISSERTATION

Mice harboring a *Pnkd* nonsense mutation associated with Tourette Disorder have behavioral abnormalities distinct from those observed in *Pnkd* knockout mice

By CARA MARIE NASELLO

Dissertation Director:

Jay Tischfield

Tourette Disorder (TD) is a complex neurodevelopmental disorder characterized by the presence of both chronic motor and vocal tics. Psychiatric disorders, particularly Attention Deficit Hyperactivity Disorder (ADHD) and Obsessive Compulsive Disorder (OCD) are often comorbid. Despite the fact that TD is heritable, a specific genetic cause of TD has not been discovered. This is likely because multiple genes are involved, but common molecular pathways are affected. Whole exome sequencing analysis of an extended TD pedigree revealed a heterozygous segregating nonsense mutation in the PNKD gene (c.415C>T) in affected individuals. The PNKD gene has at least three alternatively spliced isoforms (short, medium, and long) with differential tissue expression and cellular localization patterns.

Previously we reported that human neurons derived from induced pluripotent stem cells (iPSC) of two members of the TD pedigree heterozygous for the *PNKD*c.415C>T nonsense mutation had both reduced levels of PNKD and reduced levels of the synaptic active zone protein, RIMS1. RIMS1 regulates Ca^{2+} induced neurotransmission. Ptacek

et. al. 2014 previously reported that PNKD stabilizes RIMS1 protein at the presynaptic terminal. Because RIMS1 is critical in the regulation of neurotransmission and PNKD-long stabilizes RIMS1, we hypothesized that haploinsufficiency of the PNKD-long isoform causes reduction of RIMS1 in subjects heterozygous for the *PNKD*c.415C>T nonsense mutation resulting in TD symptoms within the studied TD pedigree.

To further investigate the role of the *PNKD*c.415C>T nonsense mutation in the etiology of TD, we created mice which harbored the same nonsense mutation using the CRISPR/CAS9 genome modification system. Additionally, we studied *Pnkd* knockout mice which were readily available through Jackson labs. We performed behavior and molecular studies on both groups of mice. We hypothesized that both mutant Pnkd-long and -medium alternatively spliced mRNA transcripts with the early translation termination codon would be rapidly degraded through nonsense mediated decay. Because of this, we anticipated mice harboring the *Pnkd*c.415C>T nonsense mutation would have the same phenotype as *Pnkd* knockout mice. However, we report here that the mutant Pnkd-medium mRNA transcript is stable while the mutant Pnkd-long transcript is rapidly degraded. Additionally, distinct behavioral differences were discovered between homozygous *Pnkd*c.415C>T mice and homozygous *Pnkd* Knockout mice**. Due to these findings, we propose an alternative hypothesis postulating that a stable mutant Pnkd-medium isoform may be the cause, or a contributing factor to the TD phenotype in the family studied. Alternatively, haploinsufficiency of Pnkd-long, expressed only in neurons, as well as an aberrantly expressed mutant -medium isoform may each play a separate role in the etiology of TD and possibly OCD and/or ADHD within this multigenerational pedigree.**

ACKNOWLEDGEMENTS

There are many people who made this dissertation possible. First and foremost, I thank my dissertation advisor, Dr. Jay Tischfield, who believed in me more than I believed in myself and without whose support this would not have been possible. I also thank my thesis committee as well as lab members, particularly for their support and guidance. I particularly thank the lab manager Lily Deng, as well Christopher Zhao who dedicated 3 of his undergraduate years to this project.

I also thank my family for putting up with me through probably one of the longest PhDs on record: Elcin Yildirim, my other half, who beared the brunt of all of my stress and uncertainty but never lost faith in me. My twin sister, Diana, my parents and both of my brothers, Adam and Brett. Without who I would not be here. I would also like to thank the many friends I met along the way particularly Julie Maguire, Piya Ghose, and Berta Vasquez.

A special thanks to my Grandmother, Marie Scara, who through her dedication to both her lifelong career and her family was the best role model possible.

DEDICATION

To both of my Grandmothers, Marjorie Roth and Marie Scara

TABLE OF CONTENTS

LIST OF TABLES

LIST OF FIGURES

Chapter 1 Figures:

Chapter 2 Figures:

BACKGROUND AND RESEARCH OBJECTIVES

Tourette Disorder (TD) is a complex juvenile onset neurodevelopmental disorder. Chronic tics, both motor and vocal are the defining feature of TD. Tics can be distinguished from other motor disorders in that their onset is often predictable and temporarily suppressible (Bronfeld et al., 2013). Tics are defined as semi-voluntary movements which are sudden and repetitive and can at times appear purposeful. Tics can be simple or complex. Simple tics, such as shoulder shrugging or throat clearing, involve only one muscle group while complex tics involve multiple muscle groups. Complex vocal tics include echolalia (repetition of vocalizations), palilalia (repetition of words and phrases) or coprolalia (repetition of obscene or inappropriate language). Although coprolalia is the most publicly recognized feature of TD, only roughly 20% of patients with TD experience this symptom (Eapen, 2015).

The exact prevalence of TD is not known, but it likely affects between 0.4-1% of the population (Bronfeld et al., 2013; Paschou, 2013). A significant gender bias exists in TD. Boys are diagnosed at a ratio of 4:1 in comparison to girls. The course of TD varies widely between individuals but the highest severity of tics is commonly observed in children between the ages of 10-12 years of age. A majority of patients experience a reduction in tic severity as young adults (Bronfeld et al., 2013; Leckman et al., 1998; Paschou, 2013).

Studies of familial presentation of TD have confirmed its heritability. Diagnoses of TD are concordant in 50% of monozygotic twins. Concordance drops to 8% in dizygotic twins. Additionally, chronic motor tics, a related disorder in which only motor but no vocal tics exist, presents with a concordance of 77-96% in monozygotic twins

and only 23% in dizygotic twins (Felling and Singer, 2011; Paschou, 2013). Despite this apparent heritability, no common underlying genetic cause has been discovered. This is likely due to the heterogeneity of TD. Tic severity varies tremendously between individuals both during childhood and adulthood. Additionally, environmental and epigenetic factors likely play a role in onset (Cauchi, R and Tarnok, 2012; Paschou, 2013). Despite these complexities, linkage analysis has led to the discovery of multiple gene variants associated with TD.

In the DSM-V, TD is categorized as a neurodevelopmental disorder; however, it is a complex disorder which blurs the boundary between a neurodevelopmental and a neuropsychiatric disorder. Strikingly, about 90% of those diagnosed with TD are afflicted with a comorbid neuropsychiatric or neurodevelopmental disorder (Hirschtritt et al., 2016; Paschou, 2013). The two most common comorbidities are ADHD which presents in up to 60% of cases and OCD which presents in 45-60% of cases (Paschou, 2013). In a study of 1300 subjects diagnosed with TD and 1100 unaffected family members conducted between 1992-2008, it was found that about one-third of TD affected participants were diagnosed with both ADHD and OCD. Additionally, as much as 72% of individuals with TD had either ADHD or OCD. While ADHD and OCD are considered the core psychiatric comorbidities in TD, other neuropsychiatric and neurodevelopmental comorbidities are significantly more prevalent in subjects diagnosed with TD in comparison to unaffected individuals. Roughly 30% of TD patients have comorbid mood disorders (including major depressive disorder, bipolar disorders, and dysthymia), anxiety disorders other than OCD, or disruptive behavior disorder. Furthermore, a diagnosis of TD independent of OCD or ADHD leads to a

significant increase in the risk of developing an anxiety disorder. Therefore, the majority of children diagnosed with TD will be expected to develop at least one comorbid psychiatric disorder, and more than 50% can be expected to develop at least two (Hirschtritt et al., 2016).

Neurodevelopmental disorders are also at an increased prevalence in TD. Recent studies have focused on a possible connection between autism spectrum disorders (ASD) and TD. In a report published in 2016, it was found that 20% of subjects diagnosed with TD also qualified for an ASD diagnosis while only 3.2% of their unaffected family members did (Huisman-van Dijk et al., 2016a). Additionally, rare CNVs associated with TD have significant overlap with those associated with ASD (Fernandez et al., 2012). The comorbid presentation of these neurodevelopmental and neuropsychiatric conditions with TD suggest shared pathophysiology and genetics between these symptomatically distinct conditions. The presence or absence of specific comorbid conditions emphasizes the heterogeneity of TD and the need to move away from viewing it as a single categorical disorder to being part of a wide spectrum of conditions.

Various etiological factors have been hypothesized as causes of TD. TD has a high degree of heterogeneity between individuals suggesting that the specific cause may be unique between most individuals although common aberrant pathways may be shared. There is strong evidence that the basal ganglia, a discrete set of nuclei in the mid-region of the brain that regulates both voluntary and involuntary movements, are directly involved. The basal ganglia includes the striatum, the subthalamic nucleus, and the globus pallidus internal and external (Macrì et al., 2013). These structures modulate

cortical excitability and form the cortico-striatal-thalamo cortical (CSTC) loops of which disruptions may be a major underlying cause of TD (Bronfeld et al., 2013; Godar et al., 2014). The prefrontal cortex, part of the CSTC loop, may be critical in the ability of individuals to suppress tics (Godar et al., 2014). In support of a direct role of CSTC loops in the etiology of TD, post mortem brain tissue of individuals with TD were found to have decreased volume in both the striatum and globus pallidus (Bronfeld et al., 2013).

Multiple neurotransmitters act within the CSTC loop and may play a role in TD. The "dopamine hypothesis" states that excessive dopaminergic activation in patients with TD causes symptoms. This hypothesis was first put forth in the 1970s after it was discovered that antipsychotics, which act as dopamine receptor antagonists, help alleviate tics in some TD patients. Additionally, treatment with dopamine receptor agonists, such as amphetamines, has been shown to exacerbate tics in certain subjects (Denys et al., 2013). Studies have both supported and rebuked this hypothesis. Alterations in dopaminergic signaling within the CSTC loops have been found in individuals with TD. Imaging studies of subjects with TD show an increased density of dopamine D2 receptors, increased activation of the dopamine transporter (DAT) as well as increased phasically-released dopamine (Bronfeld et al., 2013; Obeso et al., 2014). Other studies have failed to observe any differences in dopaminergic signaling between TD subjects and control individuals.

Although, dopaminergic signaling has been the focus of many studies investigating the cause of TD, other neurotransmitters have also been implicated, including both noradrenergic and serotonergic transmission. In one study, adults with TD had

increased levels of norepinephrine in their cerebral spinal fluid, and excreted significantly higher levels of norepinephrine in their urine in response to stress when compared to unaffected individuals. Significantly, treatment with drugs which specifically target the alpha2-adrenergic receptor which binds norepinephrine, such as clonidine, effectively reduces tic severity and additionally reduces ADHD symptoms in some subjects suffering from both TD and ADHD (Leckman et al., 2010). However, the presence of ADHD may be required for noradrenergic signaling modulation to be an effective treatment for tics supporting the view that despite the fact that the core symptom of TD is tics, pathophysiology may vary between individuals (Macrì et al., 2013).

Alterations in serotonin transmission are present in at least some individuals with TD. Subjects with TD were found to have reduced tryptophan, the precursor of serotonin, in both blood and post-mortem brain samples. Changes in expression of the serotonin transporter protein (SERT), due to promoter variants has been associated with TD and other neuropsychiatric disorders, including depression and OCD. Additionally, a gain of function missense mutation, I425V, was found to be more prevalent in subjects affected with TD (1.57% compared to 0.15%). The I425V mutation combined with expression of a specific promoter variant already associated with major depression disorder results in a hyperserotonergic condition which may upregulate expression of the serotonin receptor 5-HT_{2A} post-synaptically resulting in increased dopaminergic transmission (Moya et al., 2013). Despite these data, drugs which modulate serotonin signaling have not been effective in most instances of TD for which they were tried. These negative clinical results bring to question a direct role for serotonin in the

pathophysiology of TD. Alternatively, it may display, like the studies on noradrenergic signaling mentioned above, that basic pathophysiology in many cases may be unique despite similar symptomatology.

In addition to neurotransmitters, the cellular make-up of the brains of subjects with TD may be fundamentally altered in comparison to unaffected individuals. Postmortem sampling of affected individuals has shown a decreased number of interneurons in the basal ganglia (Kalanithi et al., 2005). A study in mice found that ablation of interneurons resulted in an increase in tic-like stereotypy behavior in mice, further supporting a hypothesis for changes in cellular content in the basal ganglia of TD patients (Xu et al., 2015).

Use of animal models to study TD

The heritability of TD makes the use of genetic animal models appealing. Such models have already helped disentangle some of the biological pathways that are key to our understanding of TD pathophysiology. Multiple mouse models of TD which recapitulate at least part of the observed phenotype in humans have been created. One well-studied example, is the *Hdc* knockout mouse, which exhibits behavioral phenotypes similar to those of TD-affected members of a family who have a segregating dominant negative mutation in the *HDC* gene. Additionally, these mice react to treatment with antipsychotic drugs supporting a role for dopamine signaling in TD (Castellan Baldan et al., 2014).

Since specific genes associated with TD have been identified in only a small number of affected individuals, and the specific etiologies of the disorder are not known, the validation of putative pre-clinical animal models with TD is challenging. The research

domain criteria (RDoc) proposed by the National Institute of Mental Health may be a better scheme to study animal models of TD, as it does not require a known etiology or an expected response to a drug treatment (Insel et al., 2010; Kozak and Cuthbert, 2016; Patrick and Hajcak, 2016). RDoc was launched in the hope of further advancing our mechanistic knowledge of neuropsychiatric disorders and improving the medical treatment of mental disorders, including TD (Insel et al., 2010; Kozak and Cuthbert, 2016; Patrick and Hajcak, 2016). RDoc attempts to change the way in which complex mental disorders are studied and diagnosed. Rather than using the traditional approach in which an individual must display at least a subset of a list of subjective symptoms for a diagnosis, RDoc is a dimensional approach in which observable behaviors and neurobiological measures are used for the classification of brain disorders.

The original diagnostic criteria for TD dating back to the 19th century reads much like the checklist of symptoms required for the diagnosis of TD in the current Diagnostic and Statistical Manual of Mental Disorder Volume, the DSM-V (Goetz et al., 2001). The similarity between diagnostic criteria for TD, first described by Gilles de la Tourette, and those of the DSM-V underscore just how little the diagnosis of mental disorders has changed over time. Just as Gilles de la Tourette based his diagnoses of TD on a checklist of symptoms so does the DSM-V. Unfortunately, this approach has frequently hampered the study of mental disorders due to a lack of focus on underlying biological mechanisms (Kozak and Cuthbert, 2016; Patrick and Hajcak, 2016).

RDoc was created to move away from symptom checklists and towards testable "units of analysis." It was originally conceptualized for use in the clinic, but currently it

primarily serves as a guideline for pre-clinical research (Insel et al., 2010). RDoc has five major domains which each have multiple constructs (Table 1). These constructs must be measurable by any of eight units of analyses: gene, molecules, cells, circuits, physiology, behavior, self-report, or paradigms creating a matrix for the clinician or researcher to follow. These measurable dimensions can be classified along a spectrum from normal to severe allowing data to be collected on a gamut of individuals (Patrick and Hajcak, 2016).

Table 1: Domains and Constructs of RDOC

Domains	Constructs
Negative Valence Systems	Acute threat, Potential threat, Sustained threat, loss, Frustrative non-reward
Positive Valence systems	Approach motivation, Initial responsiveness to reward, Sustained responsiveness to reward, Reward learning, Habit
Cognitive Systems	Attention, Perception, Declarative memory, Language behavior, Cognitive control, Working memory
Systems for social processes	Affiliation and attachment, Social communication, Perception and understanding of self, Perception and understanding of others
Arousal and Regulatory systems	Arousal, Circadian rhythms, Sleep and wakefulness

The large overlap of genetic risk factors between different mental disorders makes the parsimonious diagnostic approach used by RDoc attractive. The frequent occurrence of comorbidities in individuals affected by mental disorders, such as with TD, and overlapping symptoms between disorders complicates both treatment and diagnosis, which RDoc can potentially help simplify. In a 2013 study of 33,000 individuals with either Autism Spectrum Disorder (ASD), Attention Deficit Hyperactivity Disorder (ADHD), Bipolar Disorder, Major Depression or Schizophrenia, shared genetic risk

factors were found (Adam, 2013; Smoller et al., 2013). As with these disorders, TD is a complex disorder frequently comorbid with other mental disorders such as OCD and ADHD (Huisman-van Dijk et al., 2016b; Leckman et al., 1998; Paschou, 2013). In a genome wide analyses of subjects with TD alone, OCD alone, and TD with comorbid OCD, no specific genetic variant was associated with the TD-OCD phenotype. Furthermore, polygenic analyses to determine if multiple gene variants of small effect are causative of TD and OCD revealed distinct genetic architecture between the two disorders. Cases of OCD alone were predictable using polygenic analysis while cases of TD were not, although this may have been due to a smaller sampling of TD cases. However, polygenic analyses of cases of TD with comorbid OCD reduced the predictability of determining cases from controls in comparison to cases of OCD-alone and TD-alone further supporting genetic heterogeneity of TD and OCD (Yu et al., 2015). Therefore, it is imperative to view complex disorders, such as TD, not as a disorder substantiated by a specific list of symptoms but as part of a spectrum of overlapping conditions. By using RDoc constructs, we can directly measure behavioral phenotypes in animals on a spectrum from normal to severe as well as determine molecular mechanisms through the testable units of analysis specified in RDoc. However, due to our current lack of knowledge, RDoc cannot yet be expected to fully replace DSM criteria, but it can be used in preclinical research to study the underpinnings of mental disorders in order to gain a better understanding of pathophysiology in the hope of treatment improvement in the future (Cosgrove et al., 2016a). This is a particularly important consideration in disorders such as TD, in which the etiology and symptoms varies between affected individuals.

As reviewed earlier, RDoc ignores the categorical diagnostic criteria used in the DSM-V, and instead investigates mental disorders based on five domains which are broken down into more specific constructs. Review articles have already been published on the use of RDoc in the study of preclinical animal models of other mental disorders including bipolar disorder, schizophrenia, and eating disorders, all of which are complex disorders like TD (Cosgrove et al., 2016b; Lutter et al., 2016; Sarnyai et al., 2011). In this dissertation, focus will be on investigating the behavioral phenotypes of mouse genetic models of TD (*Pnkd* knockout and *Pnkdc.417C>T*) using units of analyses within RDoc domains and constructs (Table 2).

Table 2: RDoc behavioral units of analyses relative to Tourette and related disorders

RDoc Domain	Construct	Animal Behavior Paradigm
Positive Valence Systems	Habits (tics), Compulsions	Observation of "tic-like" behavior and stereotypies, grooming, marble burying task
Negative Valence Systems	Anxiety, Phobia, Fear	Elevated plus maze, open field, fear conditioning
Cognitive Systems	Startle, Learning, Attention	Elevated plus maze, prepulse inhibition

Research Objectives

The first objective of this dissertation was to investigate a causal role of the *PNKD* gene in the pathology of TD. For this purpose, we conducted a series of behavioral experiments on two mouse models. The first model used was a *Pnkd* knockout mouse model previously published (Lee et al., 2012) and the second was a CRISPR/CAS9-generated mouse with a nonsense mutation in the *Pnkd* gene (*Pnkd*c.415C>T) which results in an early termination codon in two alternatively spliced isoforms of the *Pnkd* gene (Nasello et. al, unpublished). This mutation was found to segregate with TD

affected members within an extended family (Sun et al., 2017). Both wild-type and heterozygous mice were included in all testing. Only male mice were used for behavior paradigms. Traditionally male mice have been used in behavioral studies to eliminate estrous cycle-induced hormonal fluctuations which may influence behavior. Behavioral experiments in mice have been previously used to study mouse genetic models of TD (Castellan Baldan et al., 2014).

The second objective of this dissertation was to determine why the homozygous *Pnkd* knockout mouse and homozygous *Pnkd*c.415C>T mutant mouse exhibit unique behavioral phenotypes. The *Pnkd* knockout mouse model was made by the insertion of a neomycin between exons 5 and 9 resulting in deletion of the neuronal specific Pnkd-long isoform as well deletion of the ubiquitously expressed Pnkd-medium isoform while leaving the third Pnkd-short isoform intact (Lee et al., 2012). The *Pnkd*c.415C>T SNV, within exon 6 of the *Pnkd* gene, results in an early termination codon at amino acid 139 in Pnkd-long isoform and at amino acid 115 in Pnkd-medium isoform. As with the homozygous *Pnkd* knockout mouse, Pnkd-short is left intact in the homozygous *Pnkd*c.415C>T mouse. If translated the *Pnkd*c.415C>T SNV would result in truncated protein fragments of Pnkd-long and Pnkd-medium; however, we predicted that nonsense mediated decay (NMD), a cellular mechanism for preventing the expression of abnormal proteins, would rapidly degrade both the Pnkd-medium and Pnkd-long transcript prior to translation. Because both of the homozygous *Pnkd* knockout mouse and the homozygous *Pnkd*c.415C>T have the same gene functionally deleted we predicted they would exhibit the same behavioral phenotype. Despite these obvious genetic similarities, we found the two mice each exhibit distinct behavioral

phenotypes. To find a potential explanation for these differences, RNA and protein studies were conducted on both putative mouse models. Again, wild-type and heterozygous mice were included; however, females were also utilized.

Chapter 1

A NONSENSE MUTATION AND KNOCKOUT OF THE *Pnkd* GENE RESULT IN DISTINCT BEHAVIORAL CHANGES IN MICE

1.1 Introduction

The discovery of causative genes of Mendelian disorders using whole exome sequencing (WES) of large family pedigrees has been remarkably successful (Warr et al., 2015). WES of multiplex families can also be useful in determining causative genes in heterogeneous neurodevelopmental and neuropsychiatric disorders. For example, WES has been used to find inherited mutations in families with consanguineous enrichment of autism (Yu et al., 2013). Genetic studies of multiplex families have been successful in the identification of genetic causes of TD. In 2010, through linkage analysis, a segregating nonsense mutation in the *L-Histidine Decarboxylase* (*HDC*) gene was discovered in all affected members of a two generation TD pedigree. The mutant *HDC* gene product was shown through enzymatic studies to have a dominant negative effect on the wild-type protein (Ercan-Sencicek et al., 2010). This mutation or others in *HDC* have not been identified in other TD families; however, subsequent to this study it was reported that there is an increase in copy number variants (CNV) including genes within histaminergic signaling pathways in individuals with TD, further supporting a potential role of histaminergic signaling dysregulation in TD (Fernandez et

al., 2012). Therefore, specific genetic causes discovered in multiplex families can help uncover critical molecular pathways.

We previously reported a large pedigree with TD and tic disorder transmitted between three generations shown in Figure 1 (Sun et al., 2017).

Figure 1: Extended TD pedigree with segregating *Pnkd*c.415C>T nonsense mutation

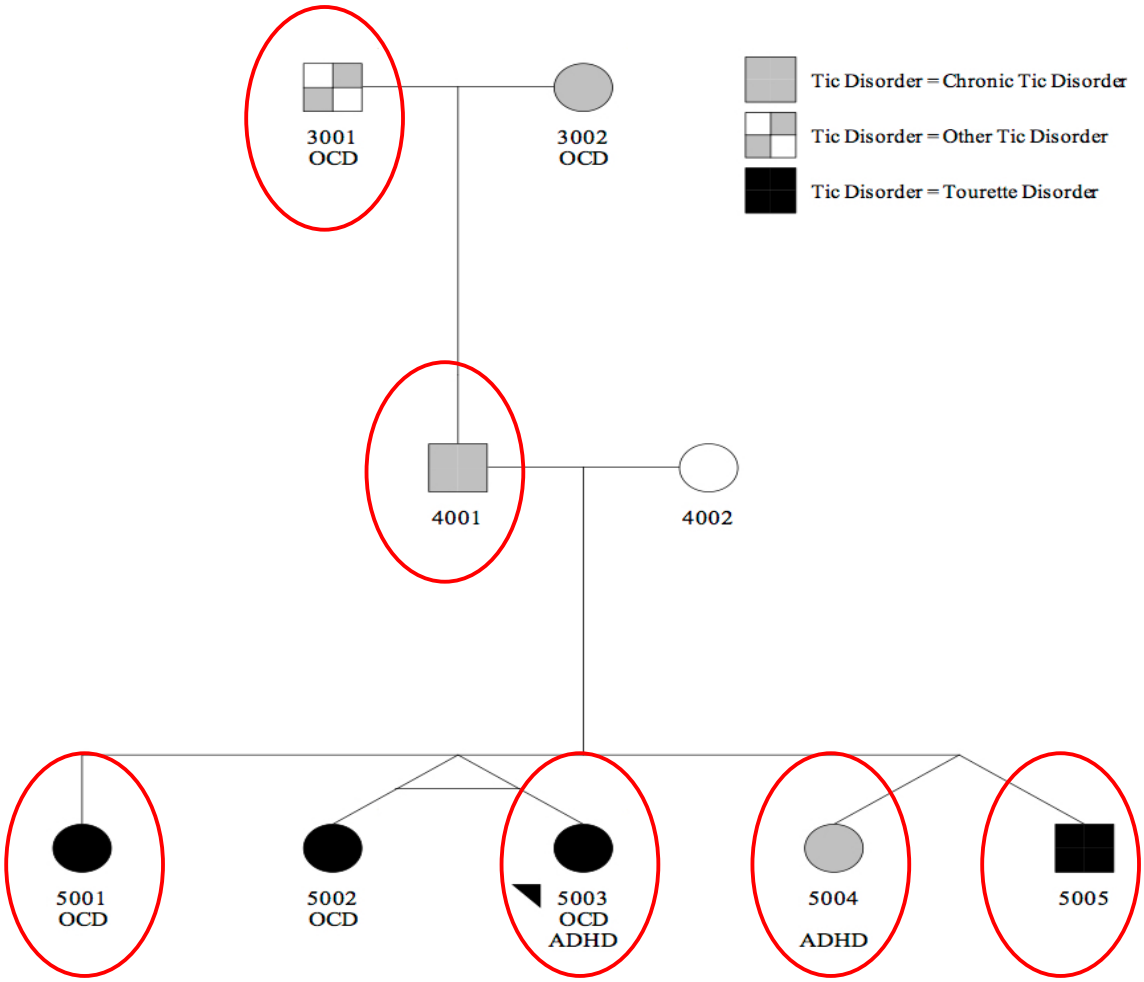

Figure 1: Multiplex TD pedigree is shown. Individuals heterozygous for the *PNKDc.415C>T* SNV are circled in red. The presence of OCD and ADHD, which are associated disorders of TD, are labelled below each individual. Circles represent females and squares represent males. Twins are indicated by diagonal lines originating from the same point, identical twins have an additional horizontal bar between bar between them (Figure modified from Sun et al, 2017).

Members of this family suffered from TD or other tic disorders and some of the members also had a diagnosis of OCD and/or ADHD. WES was completed on subjects 4001, 4002, 5001, 5003, 5004, and 5005. Since 5002 and 5003 are monozygotic twins it was assumed that they have the same genotype. This family is genetically and phenotypically complex. It is a bilineal pedigree in which both tic disorders (either chronic or not otherwise specified) and OCD are present in both maternal and paternal members of the first generation.

WES of the pedigree shown in Figure 1 revealed a segregating heterozygous nonsense mutation in the gene, *Paroxysmal Nonkinesigenic Dyskinesia* (*PNKD*). The nonsense mutation is due to a C>T transition at position chr2:219204814 which changes a codon for glutamine (CAG) to an early termination codon (TAG). pVAAST (pedigree-variant annotation analysis and search tool), a platform for determining the genetic cause of inherited disease within family members, was used to determine TD-causing gene candidates within the pedigree (Sun et al., 2017). pVAAST combines the WES data from the pedigree, background population data to determine common and rare variants, as well as potential molecular function to score likely disease causing candidate genes (Hu et al., 2014). Out of 169 genes that pVAAST scored as a potential candidate in its dominant inheritance model, *PNKD* was the top scorer (Sun et al., 2017).

While rare variants are likely to have less impact on the population in general then common variants, they can often be discovered to be causal to disease phenotypes (Yu et al., 2013). The Exome Aggregation Consortium (ExAC) database reports a frequency of 3.31×10^{-5} for the *PNKD* nonsense mutation (c.415C>T) segregating in the extended

family reported here. The *Pnkd*c.415C>T has only been observed in people of European descent at a frequency of: 6.036×10^{-5}. Furthermore, previously reported missense mutations in *PNKD* cause the rare autosomal dominant movement disorder, Paroxysmal Nonkinesigenic Dyskinesia (PNKD), suggesting a definitive role for the PNKD protein in movement control and inhibition (Sun et al., 2017).

PNKD protein has three alternatively spliced isoforms referred to as short, medium and long (Figure 2).

Figure 2: PNKD alternatively spliced isoforms with disease associated mutations

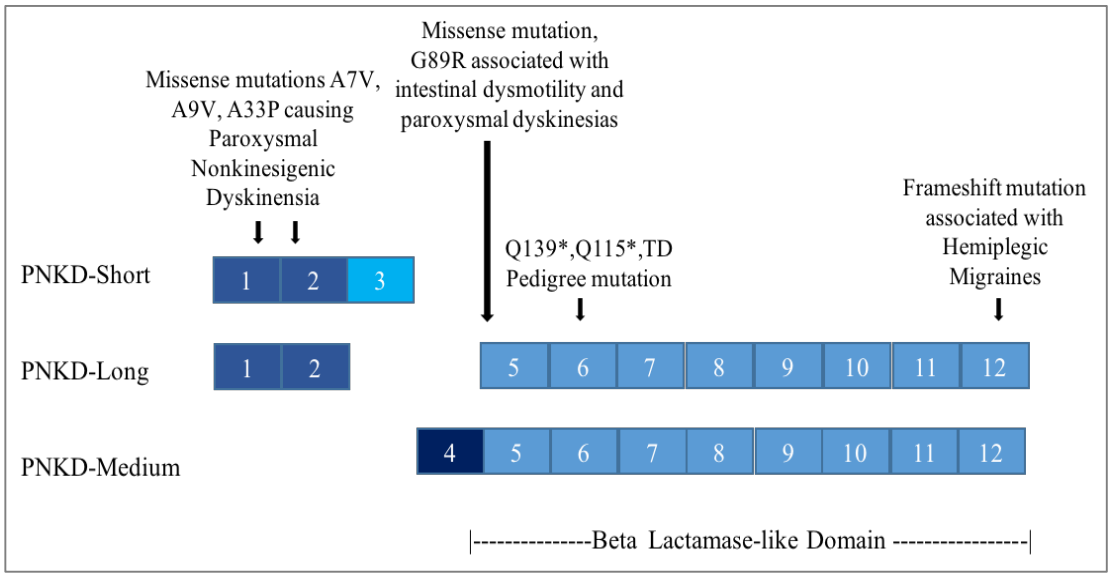

Figure 2: The transcripts of the three alternatively spliced isoforms of the *PNKD* gene showing shared and unique exons. The exonic location of disease-causing and disease-associated mutations are marked by arrows. The nonsense mutation discovered in the TD pedigree in this study is within exon 6. The location of the Beta-Lactamase-like domain is also shown.

The long, canonical, isoform is found exclusively in neurons and has been a primary focus of previously published studies of the disorder, PNKD (Lee et al., 2012, 2004, Shen et al., 2015, 2011). The medium and short isoforms are expressed in all cell types

studied. The functions of each PNKD isoform are not fully understood. The medium isoform has not been specifically investigated beyond its tissue expression(Lee et al., 2004). It shares a C-terminal domain with the long isoform, and no homology with the short isoform. It contains a unique promotor and N-terminus (Figure 2).

The short isoform, which contains exons 1-3, and shares exons 1 and 2 with the long form, has been found to function in Akt signaling in human cancer cell lines. Knockdown of PNKD short in a breast cancer cell line resulted in reduced phosphorylation of Akt at the S473 residue (Gong et al., 2014). It also appears to have a protective effect on kidney cells after renal damage by preventing recruitment of pAkt to the mitochondria (Tao et al., 2015). Although PNKD-long and -medium isoforms share homology with Hydroxyacylglutathione hydrolase, they have not been found to have any glycosylase activity (Lee et al., 2012).

Missense mutations (A7V, A9V, and A33P) within the short and long isoforms of the *PNKD* gene cause the rare autosomal dominant movement disorder, PNKD, hence the eponymous gene designation (Figure 2). PNKD is a neurological disorder characterized by involuntary movement attacks. Affected individuals have intermittent movement attacks consisting of dystonia, athetosis, and/or chorea which can last from 10 minutes to up to 12 hours. These attacks are normally triggered by caffeine or alcohol consumption but other factors such as stress or hormonal changes due to menstruation can also instigate the movement attacks. Unlike TD, in which tics may be suppressed temporarily by individuals, the movements in PNKD disorder are completely involuntary once triggered (Lee et al., 2012, 2004; Shen et al., 2015).

To further investigate the function of the mouse Pnkd gene, *Pnkd* knockout mice and *Pnkd* mutant (A7V, A9V) mice were created by Ptacek et al 2012. *Pnkd* knockout mice have exons 5-9 replaced with a neomycin-resistance cassette. Because the short isoform contains only exons 1-3, it remains intact. *Pnkd* knockout mice were not found to mimic PNKD disorder. However, knockout mice with an inserted bacterial artificial chromosome (BAC) containing the human *PNKD* gene with the disease causing mutations (A7V and A9V), displayed abnormal movements after administration of caffeine or alcohol and thus recapitulated the human disease (Lee et al., 2012).

The Pnkd-long isoform is present at both pre-synaptic and post-synaptic membranes of the frontal cortex. The Pnkd-long isoform binds Rab3-interacting molecules (RIMs) 1 and 2 in the presynaptic membrane of the frontal cortex of mice. Rims1 and Rims2 are active zone proteins that are critically important in Ca^{2+} induced neurotransmission. Rim1 and Rim2 proteins appear to have a redundancy of function, as double knockouts are embryonically lethal. Pnkd-long isoform binds RIM1 and RIM2 protein in the C2B domain shared by both isoforms of RIM. *Pnkd* knockout mice have lower levels of both Rim1 and Rim2 proteins in the frontal cortex suggesting a role for Pnkd in stabilizing Rims and, therefore, in regulating neurotransmission. Additionally, *Pnkd* knockout mice have the same, but less severe phenotype, as *Rims1* knockout mice. Like *Rims1* knockout mice, *Pnkd* knockout mice display increased paired-pulse facilitation suggesting a functional role form Pnkd at the presynaptic membrane (Shen et al., 2015).

We previously reported that neurons derived from iPSC of two of the TD-affected subjects within the extended family described herein, who were heterozygous for the

*PNKDc.*415C>T nonsense mutation, have reduced RIM1 protein levels in comparison to their unaffected mother. No significant difference in mRNA expression of RIM1 was found between the two TD-affected children in comparison to the unaffected mother. In addition to RIM1 reduction, the PNKD long isoform was also reduced in the neurons derived from the iPSC of these two affected subjects. Therefore, reduction of PNKD long protein isoform and its mRNA in human neurons was found to reduce levels of RIM1 protein just as it did in mouse cortical lysates (Sun et al., 2017).

Unique mutations in human *PNKD* have been discovered to cause distinct disease phenotypes. This could be due to instances in which one mutation results in a loss of function of the gene and another mutation results in a gain of function depending upon the location within *Pnkd* and/or the type of mutation. Different mutations in the RET gene provide an example in which different mutations within the same gene cause seemingly unrelated diseases. Loss of function mutations within RET cause Hirschsprung disorder, an inherited intestinal disease in newborns involving loss of ganglia, while gain of function mutations of the same gene lead to multiple endocrine neoplasia. Additionally, alternative splicing resulting in skipping of exons with early termination codons, as is observed in muscular dystrophy, can result in less severe phenotypes of the same disease (Prasun et al., 2007). Thus far, multiple mutations in the *PNKD* gene have been discovered in human subjects and linked to multiple disease phenotypes (Figure 2). The mutations which cause PNKD disorder (A7V, A9V and A33P) are in exons that remain in Pnkd-long and -short isoforms and are considered to be gain of function mutations (Lee et al., 2012). Another missense mutation, G89R, which is in exon 5 and therefore affects only Pnkd-medium and -long isoforms but not

the -short isoform has been linked to paroxysmal dyskinesias as well as intestinal dysmotility (personal communications with Dr. Richard Boles, Courtagen). A frameshift mutation in the last exon of the *PNKD* gene, affecting both Pnkd-medium and -long isoforms, segregated in members of a family affected by hemiplegic migraines (Gardiner et al., 2015). Because these *PNKD* mutations are associated with different phenotypes, pleiotropic functions of PNKD isoforms as well as a critical role for PNKD in neuronal function are suggested. The unique subcellular localizations of each PNKD isoform, previous evidence for distinct cellular functions, and varying expression levels of each of the three isoforms in different tissues further support a potential role for PNKD in more than one disease phenotype (Lee et al., 2004).

We wanted to determine if *Pnkd* knockout mice or mice genetically modified to harbor the *Pnkd*c.415C>T discovered in the multigenerational TD pedigree reported here exhibit any TD-associated behaviors in mouse behavioral paradigms relevant to TD. This chapter will summarize behavioral results as well as general mouse colony information regarding CRISPR/Cas9-generated *Pnkd*c.415C>T mutant mice as this was a newly generated mouse strain.

1.2 Material and Methods

1.2.1 Generation of mutant mice using CRISPR/CAS9 gene editing The Rutgers Transgenic Core Facility generated *Pnkd* mutant (c.415C>T) mice. Oocyte microinjections were done into C57/Bl6 background. A strand of synthetic RNA containing both a single guide RNA (gRNA) and CAS9 mRNA were injected together with a 120 bp DNA donor oligonucleotide containing genomic sequence of the *Pnkd*. The donor oligonucleotide contained the SNV *Pnkd*c.415C>T transition observed in the

multiplex TD pedigree we reported. Listed below are the sequences for the gRNA used and the sequence of the donor oligonucleotide. The SNV is underlined and in bold text.

gRNA sequences: 5'-CCCUGUCCUCUCGGACAACUAC-3'

Donor DNA oligonucleotide sequence:

5'-
TGAAGGTGCTTCCCATCCCTGTCCTCTCGGACAACTACAGCTACCTCATC
ATCGACACC**T**AGGCTGGGCTGGCAGTGGCTGTGGACCCCTCAGACCCGA
GGGCTGTGCAGGTGAGGGGAC-3

The tails of pups generated from microinjection were collected at 3 weeks of age and genomic sequencing was used to determine if the desired genetic change was made. Prior to sequencing, DNA was extracted and amplified using the RedExtract N-amp tissue PCR kit (Sigma, Cat. No. R4775). Each tail was incubated at 60°C overnight in 100 ml of tissue extraction solution and 25 ml of tissue preparation solution after vortexing (Sigma Cat. No. E7526 and T3073, respectively). Following overnight incubation, the lysates were each diluted 10-fold in water prior to use in PCR. Primers were designed which flanked the SNV *Pnkd*c.415C>T. The sequences of the primers used in the PCR reaction are listed in the table below (Table 3).

Table 3: CRISPR/CAS9 Mutant mouse PCR primers

Primer Name	5'->3' Sequence
Pnkd Mutant Forward	CAGCCTCTCTGTCCTCT
Pnkd Mutant Reverse	TCAGAGGAACCAGGACCAAC

The resultant PCR product was 224 bp. GoTaq DNA polymerase (Promega) was used for the PCR amplifications because GoTaq leaves TA overhangs. TA overhangs were necessary because the resultant mice from the microinjections could have unique genomic changes on each allele. TA overhangs allowed subsequent TA cloning of each allele after sequencing. Additionally, since the guide RNA, CAS9 protein and donor allele were potentially present after the single cell stage of the oocyte chimeric mice were also possible. The PCR formula for the PCR amplification of the genomic DNA is listed in the table below (Table 4).

Table 4: CRISPR/CAS9 Mutant mouse PCR reaction mixture

Reagent	Volume
5X goTaq buffer	10µl
Pnkd Mutant Forward 5uM	5µl
Pnkd Mutant Reverse 5uM	5µl
PCR nucleotide mix, 10uM	1µl
GoTaq DNA polymerase	0.25µl
Water	24.75µl
DNA	5µl
Final Volume	50µl

The PCR cycling condition for the tail lysates is listed in the table below (Table 5).

Table 5: Mouse tail lysates PCR cycling conditions:

Initial Denaturation	Amplification (35 cycles)	Final Annealing

95°C	95°C	65°C	72°C	72°C
2 minutes	30 seconds	30 seconds	45 seconds	5 minutes

Following PCR, a gel was run using 5 µl of PCR product to ensure that the expected 224 bp product was specifically produced. The PCR product was next purified using Qiagen Minelute PCR purification kit. 250 µl of buffer PB was added to each PCR product and mixed through gentle pipetting. The samples were then pipetted into a Minelute column and spun in a microcentrifuge at room temperature for one minute at 13,000 RPM. The flow through was discarded and 700 µl buffer PE was added to each sample. The columns were spun again at room temperature for one minute at 13,000 RPM and the flow through discarded. In order to dry out any excess buffer the columns were spun again at room temperature for one minute at 13,000 RPM. Following this spin, the columns were placed in clean microfuge tubes. DNA was eluted by pipetting 25 µl of nuclease free water into the center of the column and letting stand 5 minutes at room temperature. The columns were spun at room temperature for one minute at 13,000 RPM and the eluent was kept for sequencing analysis. The concentration of DNA for each sample was determined using a Nanodrop instrument (ThermoFisher).

Following purification samples were sent out for Sanger sequencing (Genewiz South Plainfield, NJ or Genscript New Brunswick, NJ). For each sequencing reaction we used 10 µl of 2ng/µl of the purified PCR product, and 5 µl of 5uM primer. Each sequencing reaction was done with either a forward primer or a reverse primer. The primers used for sequencing were the same as those used for the amplification reaction of the tail extracts. If there were multiple PCR products detected in the sequence trace, TA

cloning was used to parse out the sequence of each allele. TA cloning was achieved using the pGEM T-Easy Vector System (Promega). Purified PCR products from each mouse were ligated into the pGEM T-Easy Vector using T4 ligase. In addition to the CRISPR/CAS9 mutant *Pnkd*c.415C>T, ligations with positive control and background control samples were also completed. The molar ratio of the PCR product to vector used in each experiment was a 1:1 ratio as suggested by Promega. The ligation reaction mixture is listed in the table below (Table 6).

Table 6: TA Cloning ligation mixture

Reagent	Mouse Purified PCR Reaction	Positive Control	Background Sample
2X ligation buffer	5µl		
pGEM-T easy Vector	1µl		
Mouse purified PCR product	Dependent on the concentration	n/a	n/a
Control Insert DNA (4ng/µl)	n/a	2µl	n/a
T4 DNA ligase (3 Weiss units/µl	1µl		
Nuclease free water	To a final volume of 10µl		

After mixing the ligation reaction tubes were incubated overnight at 4°C. LB Agar plates were prepared with 100 µg per ml Ampicillin/0.1M IPTG/50 mg per ml X-Gal. The ligation reaction was transformed into JM109 high-efficiency competent cells. 50 µl of cells and 2 µl of ligation reaction were mixed by flicking the tube, which was then incubated on ice for 20 minutes. Cells were heat-shocked for 50 seconds at 42°C in a heating block. Tubes were then returned to ice for 2 minutes after which 950 µl of SOC medium was added, followed by incubation with shaking at 200 RPM for 1.5 hours at

37°C. 100 µl of cells were then plated onto two LB Agar plates containing 100 µg per ml Ampicillin/0.1M IPTG/50 mg per ml X-Gal and incubated overnight at 37°C. The following day, 10 white clones were selected from each plate and PCR amplification was used to determine if the clone contained the *Pnkd* amplicon fragment. The same PCR protocol used for the mouse tail lysates was also used for the TA clone amplified fragments. Minelute was again used for PCR purification and DNA sequencing of the PCR fragment was done by Genewiz or Genscript.

1.2.2Mating Scheme Four homozygous *Pnkd* knockout (**5** B6.129-*Pnkd*$^{tm1Lip/}$J) male mice and eight wild-type C57/Bl6J (*Pnkd*$^{+/+)}$ female mice were purchased from Jackson Laboratories. Upon arrival each *Pnkd*$^{-/-}$ male mouse was crossed with two female *Pnkd*$^{+/+}$. The progeny from these crosses were used for breeding for behavior experiments. 10-15 breeding cages each containing one male *Pnkd*$^{+/-}$ and one female *Pnkd*$^{+/-}$ were established.

Heterozygous mutant progeny (*Pnkd*+/$^{c.415C>T}$) of the CRISPR/CAS9 generated founder mouse were used for breeding. Again 10-15 cages each containing one male *Pnkd*+/$^{c.415C>T}$ and one female *Pnkd*+/$^{c.415C>T}$.

In all mating cages pups were weaned between 23-26 days of age. Following weaning, mice were separated by sex and kept in mixed genotype cages containing 3-5 animals per cage. All mice were kept in a 12/12-hour light dark cycle and provided water and food *ad libitum*.

1.2.3 Mouse Survival Although it has been previously reported that *Pnkd*$^{-/-}$ are born at expected Mendelian Ratio of 1:2:1 from *Pnkd*$^{+/-}$ crosses we wanted to confirm this data (Lee et al., 2012). The genotypes of pups were determined at 10-12 days of age. Since

it was unknown if the SNV *Pnkd*c.415C>T effects survival, we also analyzed the genotypes of pups at 10-12 days of age from *Pnkd*$^{+/c4157C>T}$ crosses. At the time of weaning, between 23-26 days of age, it was determined if pup survival differed between genotypes.

1.2.4 DNA Extraction DNA was extracted from cut tails of pups between 10-12-day old using RedExtract N-Amp tissue PCR kit (Sigma). Each tail was incubated at 60°C overnight in 100 ml of tissue extraction solution and 25 ml of tissue preparation solution after vortexing. Following overnight incubation, the lysate was diluted 10-fold with water prior to use in PCR.

1.2.5 B6.129-*Pnkd*$^{tm1Lip/}$J Genotyping B6.129-*Pnkd*$^{tm1Lip/}$J Genotyping was completed using differential size analysis of PCR products on an agarose gel. Primers recommended on the Jackson Labs website (www.jax.org) were purchased from IDT. The primer sequences are listed in the table below Table 7).

Table 7: B6.129-*Pnkd*$^{tm1Lip/}$J genotyping primer sequences

Primer Name	5'->3' Sequence
Pnkd wild-type Specific Reverse	GCTACTTCCATTTG CACGTCC
Pnkd knockout Specific Reverse	GAGCCTGAAGCCATGTATCC
Pnkd All genotypes Forward	AAGAGGTACCCAAGCCAGGT

The PCR formula for the genotyping is listed in the table below (Table 8).

Table 8: B6.129-*Pnkd*$^{tm1Lip/}$J genotyping PCR reaction mixture

	Volume
Redextract 2X Reaction Master Mix	10 µl

Pnkd Wild-type Reverse Primer 5uM	0.8 µl
Pnkd Knock out Reverse 5uM	0.8 µl
Pnkd Common Forward 5uM	0.8 µl
DNA	4 µl
Water	3.6 µl
Final Volume	20 µl

The PCR cycling conditions are listed in the table below (Table 9).

Table 9: B6.129-*Pnkd*$^{tm1Lip/}$J genotyping cycling conditions

Initial Denaturation	Amplification (35 cycles)			Final Annealing
94°C	94°C	60°C	72°C	72°C
3 minutes	15 seconds	30 seconds	45 seconds	10 minutes

The final PCR product size as it appears on an agarose gel of the wild-type mice is 332 base pairs and that of *Pnkd* Knockout mice is 510 base pairs. Heterozygous mice have PCR products of both the wild-type mice and knock-out mice. 15 µl of each PCR product was run on a 1% agarose gel.

1.2.6 *Pnkd*c.415C>T Genotyping: Tails were lysed as described above for *Pnkd*$^{-/-}$ mouse genotyping. *Pnkd*c.415C>T is a SNV; therefore, PCR product size analysis could not be used for genotyping; therefore, PCR amplification of the region of DNA containing the SNV followed by DNA sequencing was used to genotype progeny from *Pnkd*$^{+/c.415C>T}$ crosses. The same primers used during generation of *Pnkd*c.415C>T mice were used for genotyping mice from heterozygous crosses. However, for

amplification of DNA RedExtract N-Amp tissue PCR kit was used. The PCR formula is listed in the table below (Table 10).

Table 10: *Pnkd*c.415C>T genotyping PCR reaction mixture

	Volume
Redextract 2X Reaction Master Mix	10 µl
Pnkd Mutant Forward 5 µM	1 µl
Pnkd Mutant Reverse 5 µM	1 µl
DNA	5 µl
Water	3 µl
Final Volume	20 µl

The PCR cycling conditions are listed in the table below (Table 11).

Table 11: $Pnkd^{+/+}$, $Pnkd^{+/c.415C>T}$ and $Pnkd^{c.415C>T/c.415C>T}$ mouse PCR cycling conditions

Initial Denaturation	Amplification (40 cycles)			Final Annealing
94°C	94°C	63°C	72°C	72°C
3 minutes	15 seconds	30 seconds	45 seconds	10 minutes

Following PCR, DNA was purified ahead of sequencing as described above during generation of CRISPR/CAS9-generated *Pnkd* mutant mice. Genscript (New Brunswick, NJ) was used for DNA sequencing services. Sequencing results were again analyzed using four peaks. A peak for Thymine and/or Cytosine at the site of the SNV indicated either a wild-type, heterozygous, or homozygous mutant mouse.

1.2.7 Mouse Behavioral Paradigms For each behavioral test 12-25 male mice of each genotype between 2-4 months of age were tested. Behavioral testing was done during the light cycle. Mice were brought to the behavioral testing facility one week prior to testing for acclimation. When normal distribution was achieved ANOVA was used for statistical analysis. If the data was not normally distributed the Kruskal Wallis ranking test was used for statistical analysis. Multiple comparison post-hoc t-tests were done in all cases.

Open Field Arena

The open field arena was used to check locomotion as well anxiety in mice. During testing, each mouse was individually placed in a clear Plexiglas arena 40cm X 40cm (Med Associates) The mouse's activity was monitored through beam breaks detected on a grid of infrared beams on x, y and z axes. Time was broken down into 5 minute intervals. The ratio of time spent in the center versus the periphery, time spent resting versus ambulatory time and time spent rearing were analyzed. Repeated measure ANOVA was used for distance travelled analysis and one-way ANOVA at the both the initial five minute and the final twenty minute time point.

Elevated Plus Maze

The elevated plus maze used was a Plexiglas apparatus 1 meter off of the ground in which two arms are covered and two arms are open. Mice were placed in the center of the maze always facing the same open arm. Mice were allowed to explore the maze for 5 minutes. Mouse movement was recorded using a camcorder positioned above the maze and analyzed using limelight tracking software by Coulbourn Instruments. The

time spent in each arm and the number of crossings into either the open arms, closed arms, or center area were compared between genotypes.

Marble Burying Task

Twenty black marbles were laid out in a 4X5 lattice on top of two inches of bedding in a mouse Plexiglas cage. Mice remained in the cage for 30 minutes. A blinded observer (Christopher Zhao) counted the number of marbles buried that were at least 2/3 buried by the mouse. A white noise machine was used during testing.

Prepulse Inhibition

Prepulse inhibition (PPI) was used to test for sensorimotor gating deficits in homozygous *Pnkd*c.415C>T, knockout mice, and in heterozygous mice in comparison to wild-type mice. The protocol previously described in Geyer and Dulawa, 2003 was used. The prepulse settings were 71, 77 and 81 dB. The startle stimulus was 120 dB with a fast rise time and a duration of 40 msec. The background white noise was set to 65 dB. Calibration of the audio was done using a microphone provided by Med Associates (Fairfax, VT) which sat in the cylinder. Mice were placed in a Plexiglas cylinder on top of a piezoelectric accelerometer to detect movement. Initially, 6 trials of startle stimulus were completed to check for any differences in the startle reaction without a prepulse. This was then followed by 58 trials of a pseudorandom order of prepulse + startle, no stimulus, or startle alone. There were 9 trials, each of prepulse + stimulus, 10 trials of no stimulus, and 12 trials of startle stimulus only. The next block had 6 trials of startle stimulus only to check for any habituation to the startle stimulus. Prepulse inhibition was calculated using the following equation:

$$\%PPI = 100 \times [(\text{pulse-alone}) - (\text{prepulse + pulse score})]/\text{pulse-alone score}$$

The pulse-alone score is the startle only reactions from the middle block.

1.3 Results

Pup Survival: For all crosses, mice were genotyped at 10-12 days of age. Homozygous knockout mice of both sexes from crosses of *Pnkd*$^{+/-}$ mice were born at ratios not significantly different from the Mendelian ratio of 1:2:1 at the time of genotyping (Table 12). This result was unsurprising and reported previously (Lee et al., 2012).

Table 12: *Pnkd* heterozygous and homozygous knockout mice are born at Mendelian ratios

	Expected Mendelian Ratio	Male (n=244)	Female (n=240)	Both (n=484)
Pnkd$^{+/+}$	1	1(n=62)	1(n=62)	1(n=124)
Pnkd$^{+/-}$	2	2.2(n=134)	1.7(n=104)	1.9(n=238)
Pnkd$^{-/-}$	1	0.8(n=48)	1.2(n=74)	1(n=122)
Chi Square Test Statistic (dF=2)		0.33 (p=n.s.)	5.47 (p=n.s.)	0.14 (p=n.s.)

Both female and male pups from *Pnkd*$^{+/c.415C>T}$ crosses were born at the Mendelian ratio of 1:2:1 at the time of genotyping (Table 13, n=196). At the time of weaning, between 23-26 days, no difference in survival between littermates of different genotypes was observed.

Table 13: *Pnkd*c.415C>T homozygous and heterozygous mutant mice are born at Mendelian ratios

	Expected Mendelian Ratio	Male (n=99)	Female (n=97)	Both (n=196)
Pnkd$^{+/+}$	1	1 (n=23)	1 (n=34)	1 (n=57)

Pnkd$^{+/c.415C>T}$	2	2.3 (n=53)	1.2 (n=41)	1.6 (n=94)
Pnkd$^{c.415C>T/c.415C>T}$	1	1 (n=23)	0.6 (n=22)	0.8 (n=43)
Chi Square Test Statistic (dF=2)		0.33 (p=n.s)	5.27 (p=n.s)	2.21 (p=n.s)

Although *Pnkd*$^{+/c.415C>T}$ crosses had a trend for smaller litters than *Pnkd*$^{+/-}$ crosses (Student's unpaired t-test p=0.15), the difference was not significant.

Behavioral Paradigms: For all behavior experiments there were two groups of animals studied. The two groups were not studied at the same time due to timing of the availability of animals. Group one consisted of wild-type, heterozygous and homozygous *Pnkd* knockout mice (referred to in figures as +/+, +/-, and -/-, respectively). Group two consisted of wild-type, heterozygous and homozygous *Pnkd*c.415C>T mutant mice (referred in figures as +/+, +/C>T and C>T/C>T, respectively) . The data for each group will be presented separately for each behavioral paradigm and compared in summary at the end of each section. In cases in which there was a non-normal distribution as determined by the Shapiro-Wilkes Test, the Kruskal Wallis Ranking test was used, otherwise one-way ANOVA was used to determine significance between genotypes. Post-hoc multiple comparisons tests were used for pairwise comparisons.

Open Field Arena The open field arena is an "avoidance approach task" in which the mouse's need to forage and explore a novel environment competes with the natural urge to avoid an exposed space. The open field arena is a versatile test and can be used as a measure of multiple behavioral phenotypes. It measures novel environment exploration, general locomotor activity, and "anxiety-like" behavior in rodents (Bailey

KR and JN, 2009). This test has been used for mouse models of TD as well as ADHD. Before the discovery of a mutation in the *HDC* gene in a large TD human pedigree, *Hdc* knockout mice were studied to better illuminate the functional role of the Hdc protein. *Hdc* knockout mice had reduced exploratory behavior in the open field arena (Dere et al., 2004). In a later study, Castellan Baldan et al. 2014 found that untreated *Hdc* null mice, had normal locomotor activity in the open field; however, after treatment with amphetamines wild-type animals became hyperactive while heterozygous and knockout animals' movements were attenuated in comparison. The lack of hyperactivation in *Hdc* heterozygous and knockout mice was found to be associated with an increase in repetitive stereotypies. Stereotypical behavior in mice is an accepted behavioral model for tics (Castellan Baldan et al., 2014). These two studies were conducted using two different strains of mice. The earlier study used mice with a 129/Sv genetic background while the 2014 study used a C57/Bl6 background. This could potentially account for the different result obtained between the studies in the open field arena and underscores the importance of genetic background in scoring the severity of phenotype.

As noted previously ADHD is commonly comorbid with TD (Paschou, 2013). Two members the extended family with the segregating heterozygous *PNKD*c.415C>T SNV also have comorbid ADHD (Figure 1). An example of an ADHD model with abnormal behavior in the open field arena is the *Sorcs2* null mouse. The *Sorcs2* null mouse displays hyperactivity in the open field in comparison to wild-type litter mates. Additionally, treatment of *Sorcs2* null mice with amphetamines, an agonist of dopamine receptors, has a paradoxical effect which results in reduced activity in these mice. *Sorcs2* null mice show a reduction of dopamine levels in their cortex and a decrease in

dopamine metabolism in the striatum, supporting a critical role for dopamine transmission and metabolism in the etiology of ADHD (Glerup et al., 2014). This suggests that the open field arena is an appropriate behavioral test for the study of TD animal models.

In group one (*Pnkd*$^{+/+}$, *Pnkd*$^{+/-}$, and *Pnkd*$^{-/-}$ genotypes), exploration of a novel environment was analyzed by comparing the distances travelled between genotypes. The twenty-minute testing period was broken up into 4 five minute intervals. Although both knockout and heterozygous mice trended to less activity then wild-type the difference was not significant over the twenty-minute testing period (Figure 3a, dark blue=wild-type, medium blue=heterozygotes light blue=homozygous knockout, repeated measure ANOVA ($F(2, 79)$ $p=0.060$). The most critical period for exploration in the open field is the initial five minutes; therefore, we investigated if there was a significant difference between genotypes specifically during this interval (Bailey KR and JN, 2009). *Pnkd*$^{-/-}$ mice moved significantly shorter distances in comparison to wild-type mice during the initial 5 minutes of testing as well as the following 6-10-minute block (Figure 3a, Tukey's Multiple Comparisons Test, 0-5 minute block $p=0.015$, 6-10 minute block $p=0.011$). The distance travelled by heterozygous mice trended lower than wild-type mice but was not significantly different during any of the five-minute time blocks. Overall locomotion during the complete 20-minute testing period was not significantly different between the 3 genotypes (Figure 3b, One-way ANOVA $F = (2,79)$ $p=0.196$), although the distance travelled by knockout and heterozygous mice trended lower in comparison to wild-type mice. Thus, the majority of the difference observed between wild-type and knockout was observed

within the initial ten minutes of testing, indicating a reduced exploratory urge in knockout mice.

Figure 3: Open Field Arena: Distance travelled by *Pnkd* wild-type, heterozygous, and knockout mice

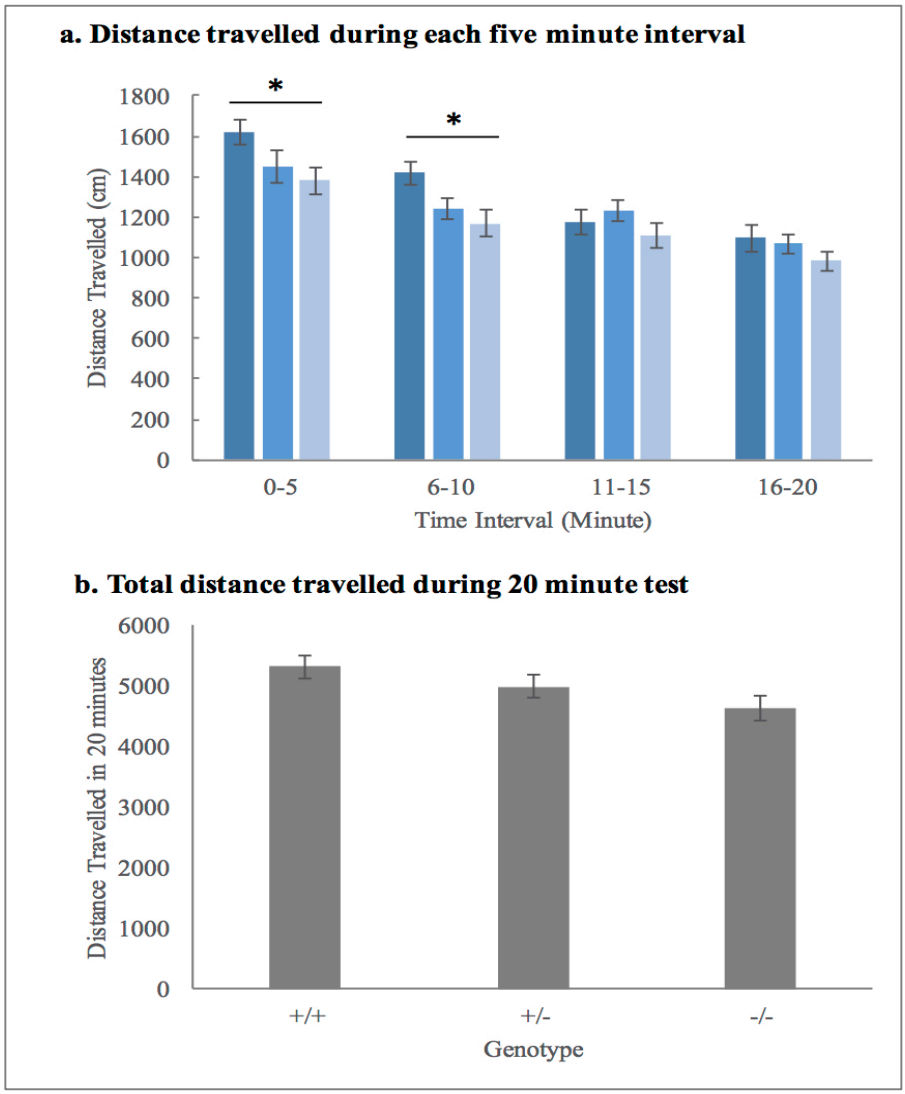

Figure 3: (a) Wild-type mice travelled significantly greater distances compared to knockout mice in the first two five minute intervals of testing (Tukey's Multiple Comparison's test, p=0.015). Repeated measure ANOVA using five minute intervals showed no significant difference between genotypes when comparing all four five minute intervals (F (2, 79), p=0.060), **dark blue=wild-type, medium blue=heterozygotes light blue=homozygous knockout** (b)Total distance travelled by each genotype over twenty minutes (n.s) +/+ n=25, +/- n=26, -/- n=31, *=p<0.05

Increased rearing in rodents is also considered to be a measure of higher exploratory urge; therefore, rearing behavior was also measured during the testing period. No differences in the time spent rearing were discovered between genotypes (Figure 4, F = (2,79), One-way ANOVA p=0.91). However, knockout mice had significantly less

rearing counts during the testing period indicating that each episode of rearing lasted longer in these mice (One-way ANOVA F (2,79) p=0.02, Tukey's Multiple Comparison's test between wild-type and knockout mice, p=0.014). This data indicates that rearing behavior was at least slightly altered in knockout mice in comparison to wild-type.

Figure 4: Open Field Arena: Rearing

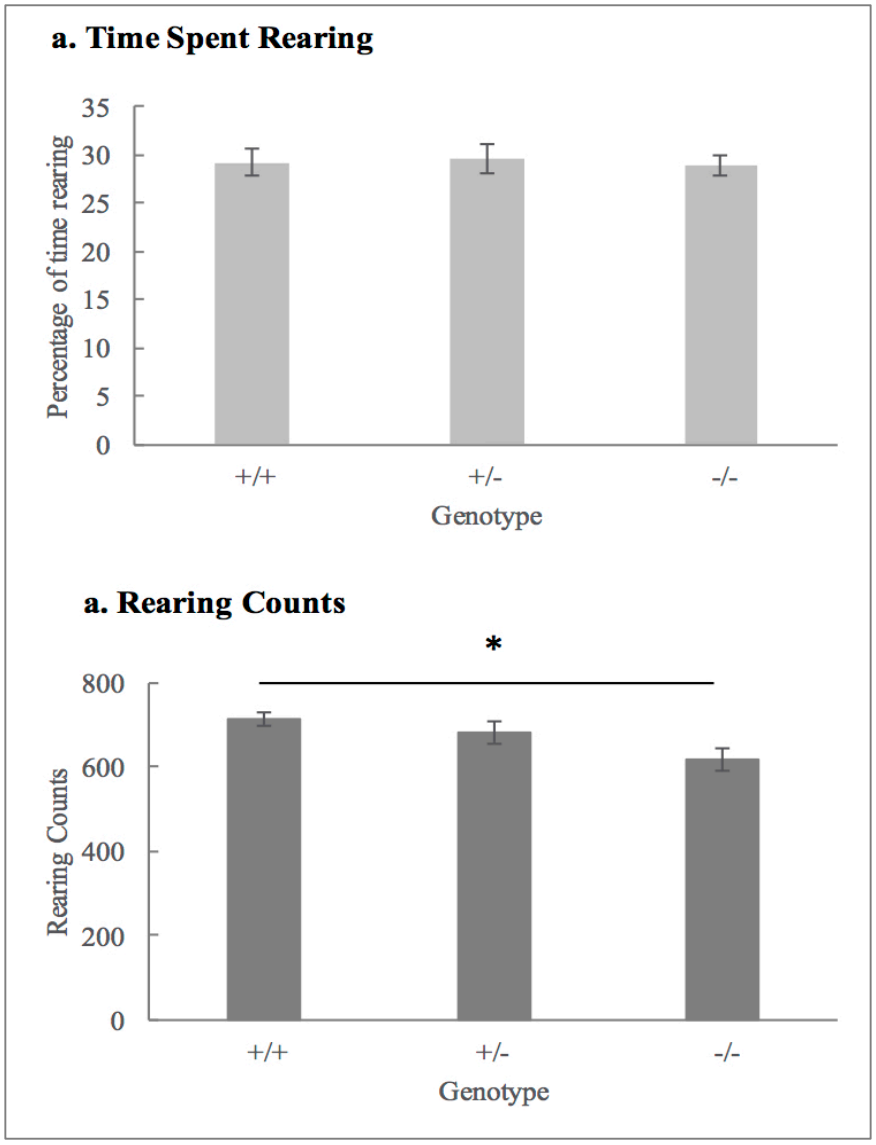

Figure 4: (a) No difference was observed between genotypes in the time spent rearing, one-way ANOVA F= (2,79), p=0.91. (b) Knockout mice had a significantly lower number of rearing bouts in comparison to wild-type (Tukey's Multiple Comparisons Test, p=0.014)
Pnkd$^{+/+}$ n=25, *Pnkd*$^{+/-}$ n=26, *Pnkd*$^{-/-}$ n=31, *=p<0.05

Group two (*Pnkd*$^{+/+}$, *Pnkd*$^{+/c.415C>T}$, and *Pnkd*$^{c.415C>T/c.415C>T}$) underwent the same testing in the open field arena as the first group. Although only marginally significant, there was a significant difference between genotypes when using repeated measures

ANOVA with five-minute time intervals (Figure 4, F (2,65), p=0.048). In contrast to group one in which the *Pnkd* homozygous knockout mice had reduced exploration during the initial ten minutes of the testing period, homozygous *Pnkd*c.415C>T were not significant different from wild-type during the first 2 five minute intervals (Figure 5a). Heterozygous *Pnkd*c.415C>T mice neared equivalence to wild-type mice in their exploration of the arena in the initial five-minute testing block, but had significantly lower activity levels during the second 6-10 minute time interval (Tukey's Multiple Comparisons Test, p=0.035) and continued a trend, although not significant for each individual interval, for lower activity during minutes 11 to 15 and 16 to 20. Over the entire testing period, heterozygous *Pnkd*c.415C>T mice were not significantly different from wild-type or homozygous mice (Kruskal Wallis Test, p~0.10, Figure 5b).

Figure 5: Open Field Arena: Distance travelled by *Pnkd* wild-type, heterozygous and homozygous *Pnkd*c.415C>T mice:

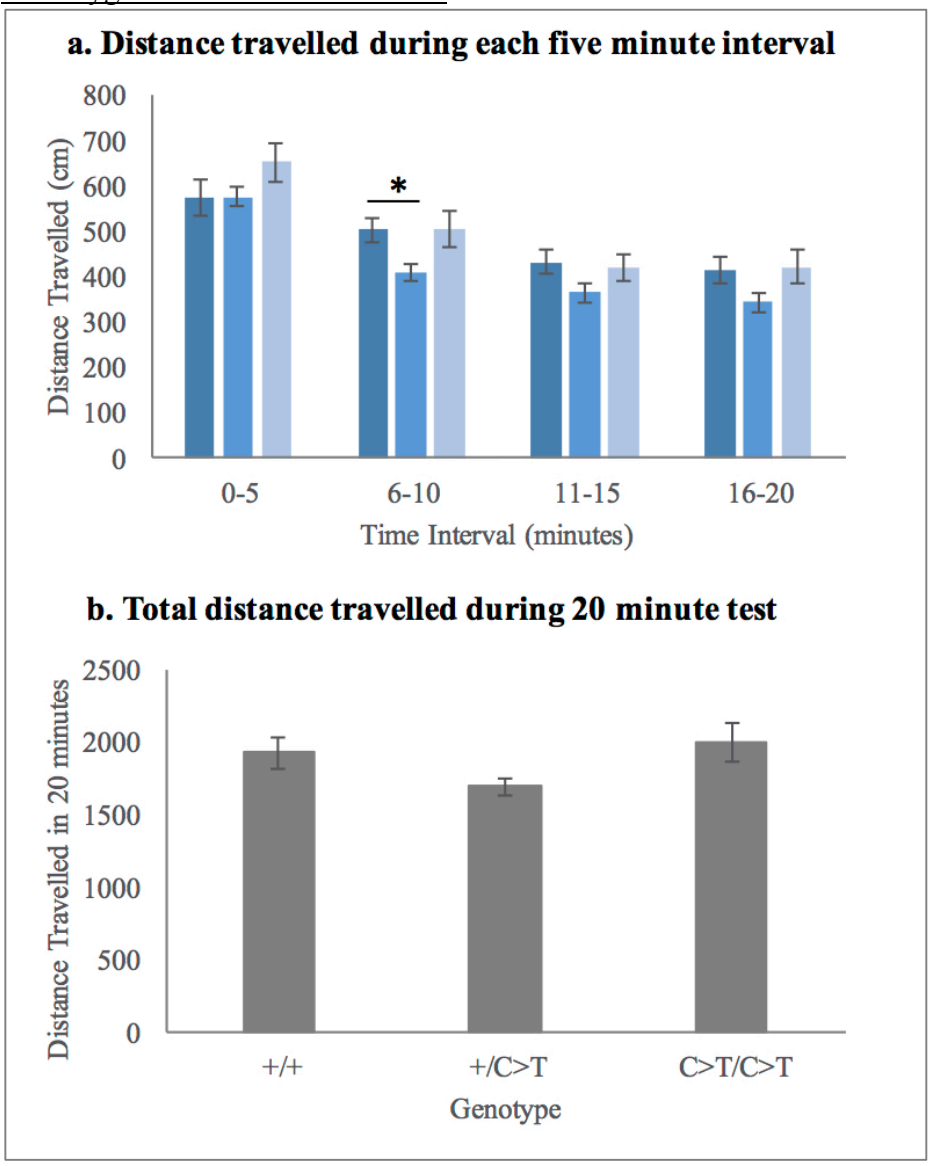

Figure 5: (a) A significant difference was found between genotypes using repeated measure ANOVA with 5 minute time intervals (main effect genotype, F (2,65) p=048). Heterozygous *Pnkd*c.415C>T mice had significantly lower locomotor activity in the 6 to 10 minute time block (Tukey's Multiple Comparisons Test p=0.035). **dark blue=wild=type, medium blue=+/C>T light blue= C>T/C>T**(b) There was no significant difference in the three genotypes using the entire 20 minute period for analysis (Kruskal Wallis Test, p=0.10) +/+ n=23, +/C>T n=29, C>T/C>T n=16, *=p<0.05

The percentage of time spent rearing as well as the number of rearing bouts was not significantly different between genotypes, although the heterozygous *Pnkd*c.415C>T

trended to spend less time rearing as well as engaging in a lower count of rearing bouts (One-way ANOVA F (2,65) p=0.13 and p=0.16, respectively).

Figure 6: Open Field Arena: Time spent rearing by *Pnkd* wild-type, heterozygous and homozygous *Pnkd*c.415C>T mice:

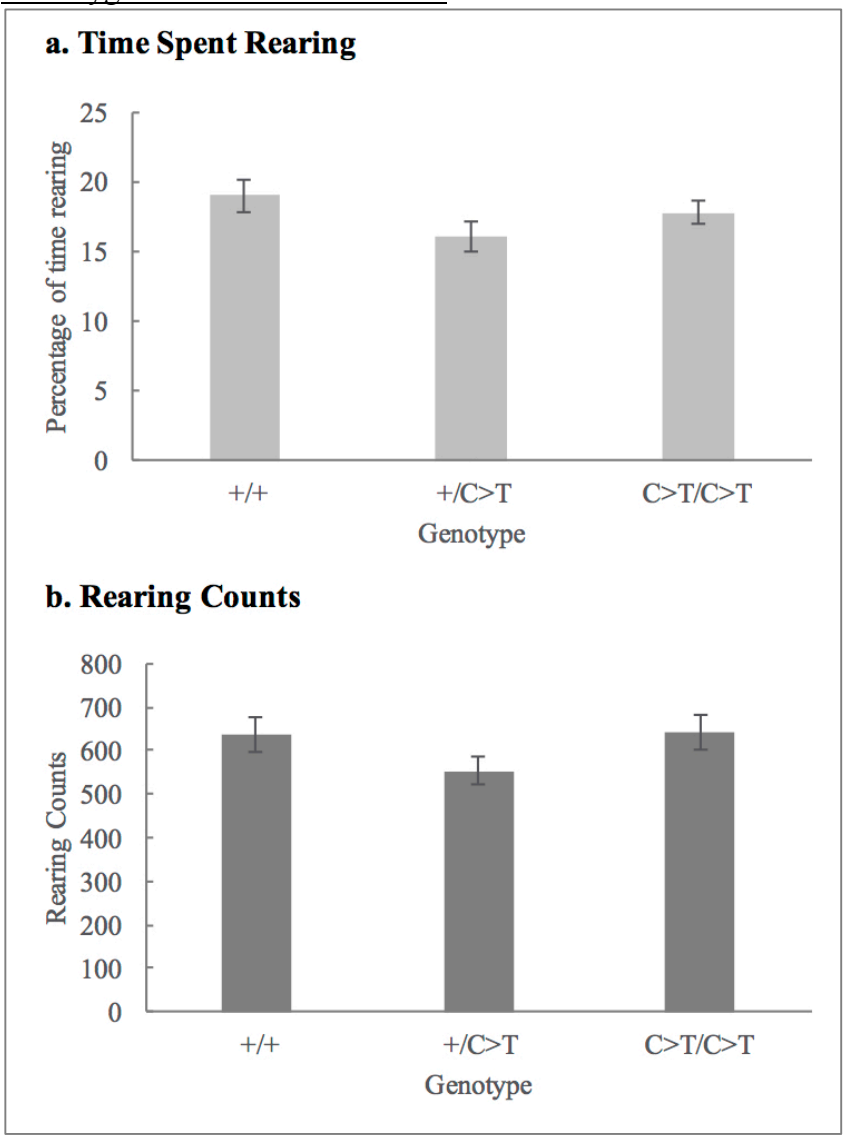

Figure 6: (a) No significant difference was found in the time spent rearing between genotypes. (b) No significant difference was found in the time number of rearing bouts between genotypes. +/+ n=23, +/C>T n=29, C>T/C>T n=16

In summary, homozygous *Pnkd* knockout mice had reduced exploration of a novel environment in comparison to wild-type mice. Heterozygous (+/-) mice were not significantly different from either wild-type or homozygous knockout mice, but their activity fell in between that of wild-type and homozygotes. When we investigated the effect of the *Pnkd*c.415C>T mutation we obtained different results from those with the knockout mice. Using repeated measures ANOVA there was a significant difference between genotypes which was primarily accounted for by heterozygous mice moving shorter distances. These results imply that the absence of Pnkd medium and/or long causes a changes in exploratory behavior in a novel environment.

In group one, *Pnkd* homozygous knockout mice had reduced exploration within the open field arena, suggesting that an "anxiety-like" or fearful phenotype was possible. Because OCD is commonly comorbid with TD and TD patients have an increased prevalence of other anxiety disorders, it would not be surprising to find an "anxiety-like" phenotype in a mouse model of TD. However, because of the heterogeneity of TD and inherent species differences, it's difficult to produce a clear hypothesis describing a mouse model's behavior in the open field. In order to further asses an "anxiety-like" phenotype in *Pnkd* knockout mouse we analyzed the proportion of time each genotype spent in the center of the arena. A large center (30X30 cm) was used for analysis and the ratio of time spent in the center to time spent in the periphery of the arena was compared. There was a significant difference between genotypes in the percentage of time spent in the center of the arena (Figure 7, Kruskal Wallis Test, $p=0.03$). *Pnkd* knockout mice spent proportionately less time in the center zone over the 20 minute testing period in comparison to heterozygous mice (Dunn's Multiple Comparisons Test,

p=0.03), but only had a trend for less time spent in the center zone in comparison to wild-type mice.

Figure 7: Percentage of time spent in the center of the open field arena by wild-type, heterozygous and knockout mice:

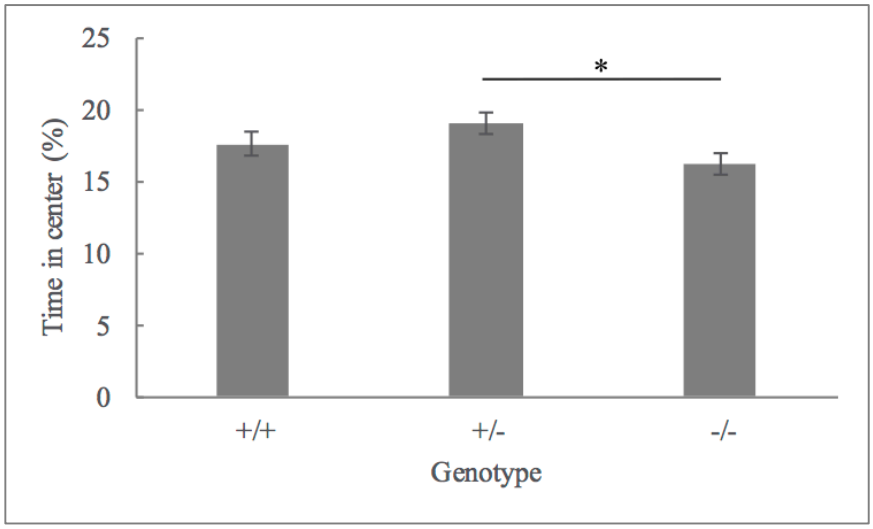

Figure 7: *Pnkd* knockout mice spent proportionately less time in the center of the arena compared to heterozygous mice (Dunn's Multiple Comparisons Test, p=0.03) but only trended lower then wild-type. Heterozygous mice were not significantly different from wild-type. $Pnkd^{+/+}$ n=25, $Pnkd^{+/-}$ n=26, $Pnkd^{-/-}$ n=31, *=p<0.05

We next determined if the presence of the *Pnkd*c.415C>T mutation resulted in a change in the proportion of time spent in the center of the arena in heterozygous and/or homozygous c.415C>T mice. There was a significant difference between the three genotypes (Figure 8, Kruskal-Wallace test p=0.027). Heterozygous *Pnkd*c.415C>T mice spent significantly less of their time in the center of the arena in comparison to wild-type mice (Figure 8, Dunn's multiple comparisons test p=0.029). Wild-type and homozygous mutant mice were not significantly different from each other nor were homozygous c.415C>T significantly different from heterozygous mice.

Figure 8: Percentage of time spent in the center of the open field arena by wild-type, heterozygous and homozygous *Pnkd*c.415C>T mice

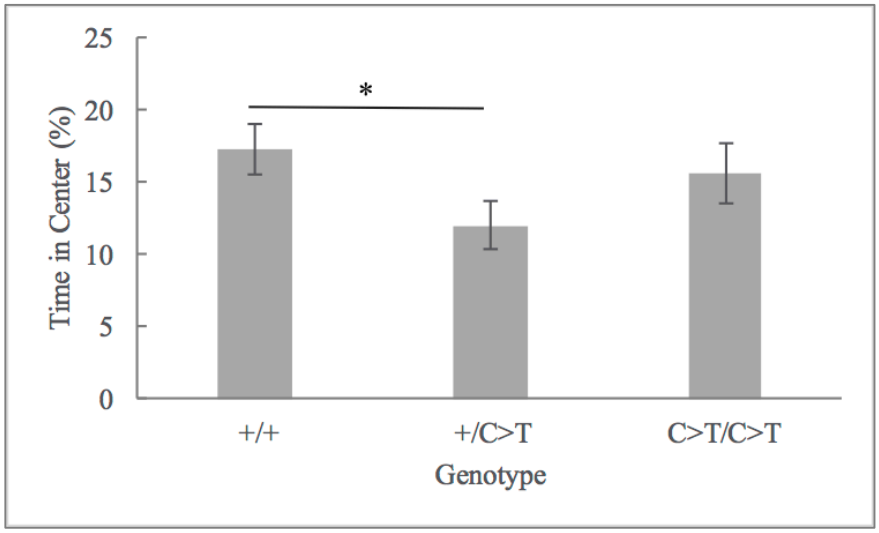

Figure 8: Heterozygous c.415C>T mice spent a reduced proportion of time in the center of the open field arena in comparison to wild-type mice (Dunn's Multiple Comparisons Test, p=0.029) but only trended lower then homozygous c.415C>T mice. There was no significant difference observed between wild-type and homozygous c.415C>T mice.
+/+ n=23, +/C>T n=29, C>T/C>T n=16, *=p<0.05

In summary, within the first group, homozygous knockout of the *Pnkd* gene appears to result in a reduced exploration upon introduction to a novel environment. In addition, homozygous knockout mice spent proportionately less time in the center of the arena suggesting increased risk evasion or higher levels of "anxiety-like" behavior. Neither of these phenotypes were severe and suggest only a minor impairment. Within the second group, heterozygous *Pnkd*c.415C>T appeared to have lower locomotor activity and spent a smaller proportion of their time in in the center of the arena. Put together, this data indicates that the *Pnkd* gene may be involved in both physical activity and emotional reactivity when a mouse is placed in a novel environment. It is interesting to note that heterozygous *Pnkd*c.415C>T mice shared a similar phenotype to

that of the *Pnkd* knockout mouse within the open field. However, one caveat of comparing the two groups is that testing of the two groups was completed more than one year apart and there were some inherent differences in activity between the wild-type mice of both groups. In particular, wild-type mice in the first group had a higher level of locomotor activity in comparison to the second group. However, these results do indicate that the *Pnkd* gene appears to be involved in response to a novel and open environment in mice.

We next investigated if any changes in behavior occurred in mice of any genotype in the elevated plus maze (EPM), another avoidance-approach task. The EPM is a plus-shaped maze one meter off of the floor which has two platform arms. Two of the arms are open and two are closed with black Plexiglas walls. Less "anxious" mice will spend more time in the open arms. However, the EPM is unable to distinguish between an increased risk-taking phenotype and a less "anxious" or more "impulsive" mouse (Steimer and Driscoll, 2003).

In addition to being used as a test for "anxiety-like" behavior in mice, EPM has also been used as a measure of "impulsive" behavior in mouse models of ADHD (Avale et al., 2004; Zimmermann et al., 2015). At the time this study was conducted, the extended TD pedigree under study also had two members diagnosed with ADHD (Figure 1). Therefore, the EPM is an appropriate behavioral test for this study. Dopamine D4 receptor (D4r knockout mice, a mouse model of ADHD) crossed significantly more times into the open arms of the EPM indicating poor behavioral inhibition, a defining characteristic of ADHD (Avale et al., 2004). Another model of ADHD, ACC ((ADF2/2/n-Cofflx/flx,CamKII-c) mice have comparable behavioral

abnormalities to the D4R knockout mice. ACC mice have the Actin Depolymerization Factor (ADF) knocked out and the adult mice have no n-cofilin in the telencephalon. Both of these proteins are highly abundant at post-synaptic synapses. ACC mice spend more time in the open arms of the elevated plus maze and cross into the open arms of the maze more frequently. Additionally ACC mice also had a tendency to jump off of the open arms indicating an even more severe impairment in risk assessment and/or increase in impulsivity in comparison to D4R knockout mice (Zimmermann et al., 2015).

In order to determine if heterozygous, or homozygous knockout mice differed in their behavior in the EPM in comparison to wild-type three parameters were measured: the ratio of time spent in the closed arms compared to the open arms, the percentage of time spent in each arm, and the percentage of the total number crossings into each of the three maze regions (open, closed, and center) during the complete 5 minute testing period. No significant differences were found between the three genotypes in the ratio of time spent in the closed arms versus the open arms of the EPM (Figure 9a, Kruskal-Wallis test $p=0.40$). The percentage of time spent in the open arms (Figure 9b, Kruskal-Wallis Test $p=0.596$) the closed arms (Figure 9b, Kruskal-Wallis Test $p=0.32$), or the time spent in center area (Figure 9b, Kruskal-Wallis Test $p=0.247$) were not significantly different. The total number of crossings into any of the maze arms did not vary significantly between genotypes (Figure 9c, One-way ANOVA $F(2,51)$ $p=0.758$). The percentage of crossings into the open arms (One-way ANOVA $F(2,51)$ $p=0.7$), closed arms (One-way ANOVA $F(2,43)$ $p=0.786$) and center (One-way ANOVA $F(2,51)$ $p=0.681$) did not vary significantly between genotypes (Figure 9d).

Figure 9: Elevated Plus Maze results for wild-type, heterozygous, and knockout mice

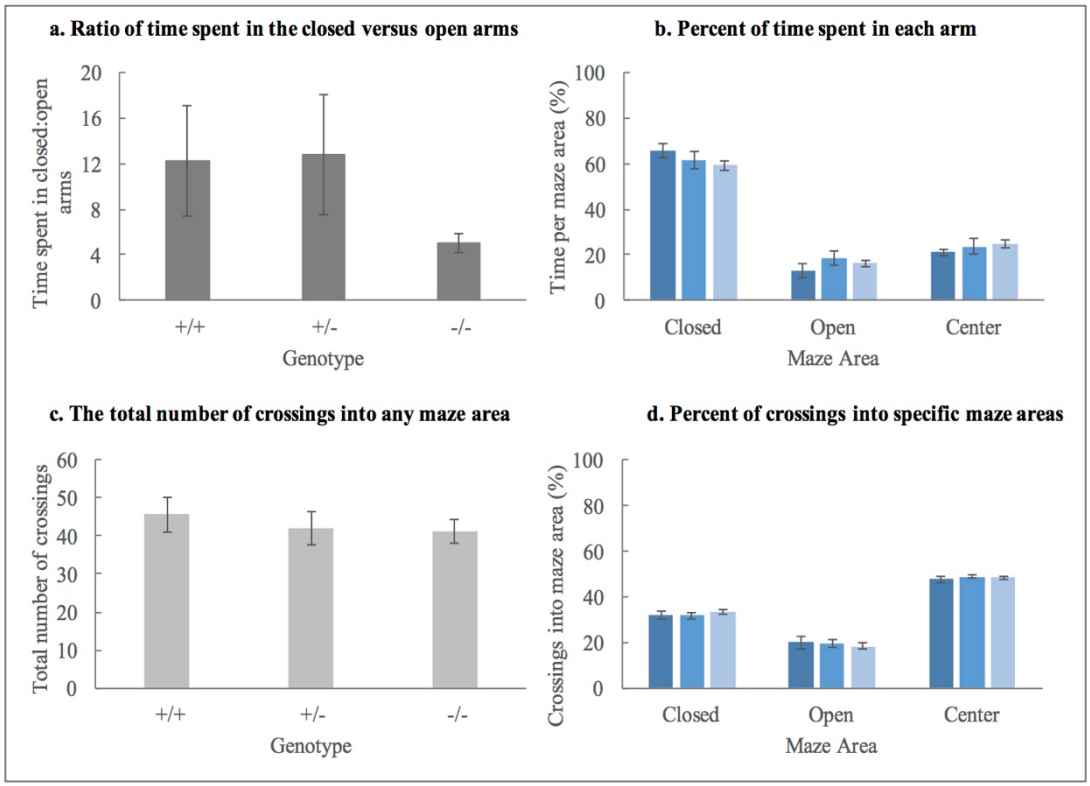

Figure 9: (a) Knockout mice had a trend of spending proportionately less time in the closed arm in comparison to both wild-type and heterozygous mice but this difference was not significant (b) The fraction of time spent in the three sections of the maze not significantly different between genotypes (c) The total number of crossings into the different sections of the EPM was not significantly different between genotypes (d) The percentage of crossings into each section of the EPM was not significantly difference was between genotypes. *Pnkd*$^{+/+}$ n=18, *Pnkd*$^{+/-}$ n=18, and *Pnkd*$^{-/-}$ n=18. **In b and d, dark blue=wild-type, medium blue=heterozygotes light blue=homozygous knockout**

In summary, heterozygous and homozygous knockout mice had no significant changes in comparison to wild-type mice in their activity within the EPM in regards to both the proportion of time spent in the open arms as well as the number of times they crossed into any of the three maze areas (open or closed arm and center). If viewed from an RDoc perspective, the EPM was not able to detect any changes in negative

valence systems (i.e., anxiety, fear) or cognitive systems (i.e., attention, impulse control).

We next investigated whether *Pnkd*c.415C>T heterozygous or homozygous mice exhibited any changes in behavior in the EPM in comparison to wild-type mice. A significant difference between the three genotypes was found in the ratio of time spent in the closed arm to the open arm (Figure 10a, One-way ANOVA F (2,39) p=0.03). Homozygous mutant mice were significantly different from heterozygous c.415C>T mice (Tukey's multiple comparisons test p=0.032). Although, there was a trend toward a reduced proportion of time in the closed arms of them maze between homozygous c.415C>T mice and wild-type mice, significance was not reached (Tukey's multiple comparisons test p =0.08). Heterozygous c.415C>T mice did not differ significantly from wild-type mice (Tukey's multiple comparisons test p=0.7). The percent of time spent in the closed arms was significantly different between genotypes (Figure 10b, One way ANOVA F (2,39) p=0.0042). Homozygous c.415C>T mice spent significantly less time in the closed arms then both wild-type and heterozygous c.415C>T mice (Tukey's Multiple Comparisons Test, p=0.013 and p=0.0073, respectively). The time spent in the open arms neared significance between genotypes (One-way ANOVA F (2,39) p=0.053). The lack of significance between genotypes in the time spent in the open arms can be accounted for by the slight, but insignificant increase in the time spent in the center by homozygous c.415C>T mice in comparison to wild-type and heterozygous c.415C>T mice. There were no significant differences in the number of crossings into the open (one-way ANOVA F (2,39) p=0.29), closed (p=0.65) or center area (p=0.1443)

between genotypes. The total number of crossings overall was also not significantly different between genotypes (One-way ANOVA F (2,39) p=0.63 Figure 10c and 10d).

Figure 10: Elevated Plus Maze results for wild-type, heterozygous and homozygous *Pnkd*c.415C>T mice:

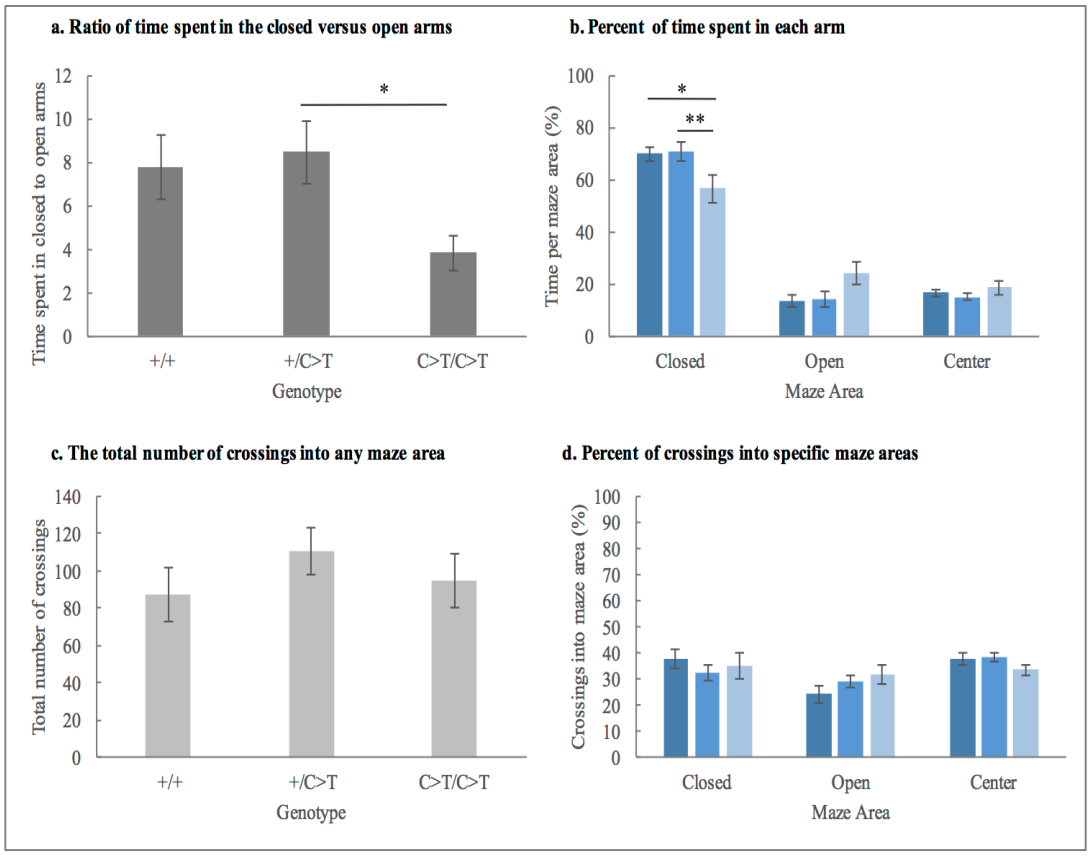

Figure 10: (a) Homozygous c.415C>T spent proportionately less time in the closed arms (One-way ANOVA between genotypes F (2, 39) p=0.03, Tukey's Multiple Comparisons test between heterozygous and homozygous c.415CC>T mice, p=0.032) (b) Homozygous mutant mice spent less time in the closed arms of the maze (One-way ANOVA F (2,39) p=0.0042, Tukey's Multiple Comparisons test between wild-type and homozygous c.415C>T p=0.013, between heterozygous and homozygous c.415C>T mice p=0.0073. There was not a significant difference in the percentage of time spent in the other areas of the maze between genotypes. (c) There was no significant difference in the total number of crossings into any maze area between genotypes. (d) There was no significant difference in the number of crossings into either the closed, open, or center areas of the maze. +/+ n=12, +/C>T n=16, C>T/C>T n=14, **In b and d, dark blue=wild-type, medium blue=heterozygotes, light blue=homozygous knockout, *=p<0.05, **=p<0.01**

In summary, of all of the genotypes tested in the EPM only the homozygous *Pnkd*c.415C>T mice showed a significant difference in the amount of time spent in the open arm in comparison to the closed arm. Although, homozygous knockout mice showed the same trend, the difference was not significant. Homozygous *Pnkd*c.415C>T mice spent less time within the closed arms, indicating that the Pnkd protein may be involved in processes affecting risk assessment. While knockout and single mutant mice appeared to be a more fearful phenotype within the open field, as these mice spent proportionately less time in the center of the arena, this phenotype was not corroborated in the EPM.

TD is frequently comorbid with OCD; and was diagnosed in four family members heterozygous for the *PNKD*c.415C>T mutation in the TD pedigree under study. Therefore, we wanted to test if homozygous and heterozygous knockout or *Pnkd* c.415C>T mice had an obsessive phenotype. To detect any obsessive or repetitive behaviors in the mice, the mice completed the marble burying task which is an established measure of compulsive behavior. During this test, mice are presented with a lattice of 20 marbles sitting atop a thick layer of bedding. The number of marbles buried is counted after 30 minutes of testing. The test studies digging in mice, which is a normal behavior, but when done excessively is considered abnormal. The excessive digging is likened to stereotypic behavior and compulsions in humans. The time spent digging and the number of marbles buried during the test are positively correlated (Thomas et al., 2009). The test has been used to study mouse models of autism, as well as for testing the efficacy of drugs developed for the treatment of OCD. Drugs

commonly used to treat OCD, such as selective serotonin reuptake inhibitors (SSRI) reduce marble burying behavior (Deacon, 2006).

A significant difference was found between wild-type, heterozygous and homozygous knockout genotypes (Figure 11, One-way ANOVA F (2,36) p=0.032). In pairwise comparisons knockout mice buried significantly more marbles then wild-type mice (Tukey's multiple comparisons test, p=0.036). The increased marble burying indicates homozygous *Pnkd* knockout mice appear to exhibit an "OCD-like" behavior in the marble burying task.

Figure 11: Marble Burying Task results in wild-type, heterozygous, and knockout mice:

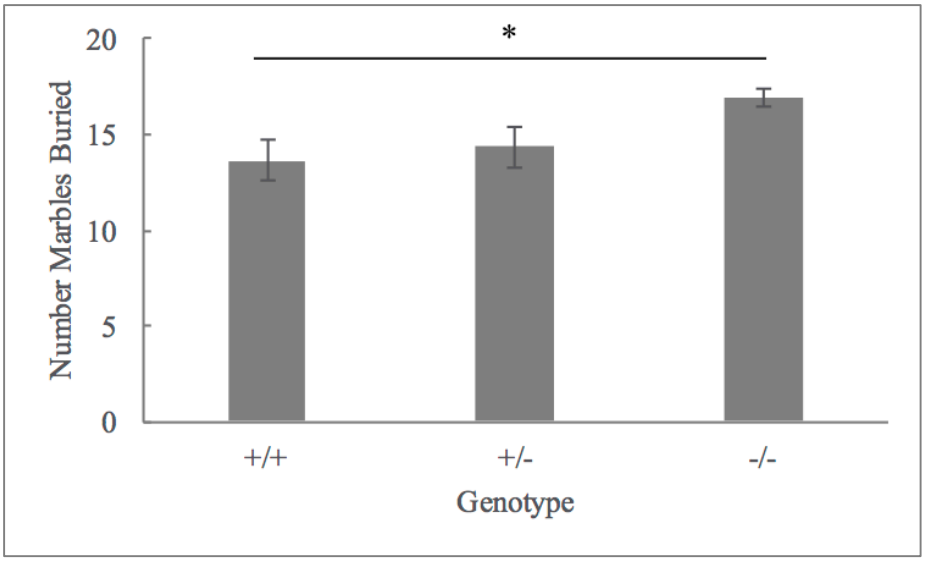

Figure 11: *Pnkd* Knockout mice bury significantly more marbles in the marble burying task in comparison to wild-type mice. (One-way ANOVA between genotypes F (2,36) p=0.032, Tukey's Multiple Comparisons Test between wild-type and knockout mice, p=0.036), +/+ n=12, +/- n=14, -/- n=13, *=p<0.05

We next tested if heterozygous and/or homozygous *Pnkd*c.415C>T mice would have a similar phenotype to *Pnkd* knockout mice in the marble burying task. No significant differences were observed between wild-type, heterozygous or homozygous

c.415C>T mice (Figure 12, One-Way ANOVA F (2, 55) p=0.44). In summary, the presence of the mutant allele did not affect mouse digging behavior while complete knockout of the *Pnkd*-medium and -long isoforms resulted in increased repetitive digging behavior.

Figure 12: Marble Burying Task results in wild-type, heterozygous and homozygous *Pnkd*c.415C>T mice:

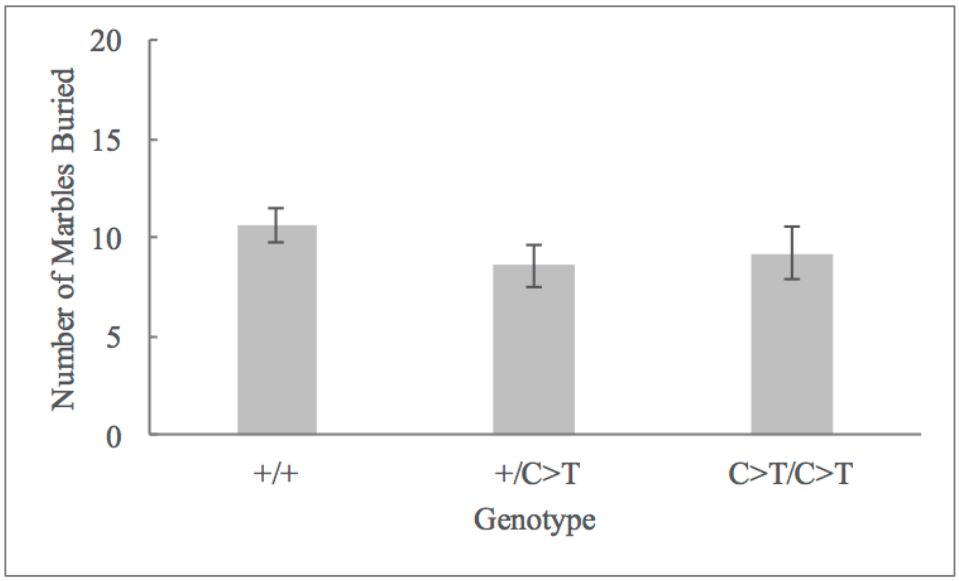

Figure 12*:* There was no significant difference in the number of marbles buried between wild-type, heterozygous or homozygous c.415C>T mice. +/+ n=17, +/C>T n=24, C>T/C>T n=17

Next we tested sensorimotor gating in both groups of mice by measuring prepulse inhibition of acoustic startle. Prepulse inhibition (PPI) is a measure of sensorimotor gating, the process by which neuronal systems screen sensory information and allow only the most necessary stimuli to go through to higher level processing. Sensory habituation is primarily controlled by reticular neurons within the brain stem. Projections of the reticular neurons reach cholinergic neurons whose projections activate inhibitory neurons in the hippocampus limiting response to repeated stimuli.

Modulation of a response to a sensory stimulus occurs through excitatory glutamatergic neurotransmitters (Javitt and Freedman, 2015). Because sensory habituation involves multiple brain regions, it seems unsurprising that prepulse inhibition deficits are observed in multiple mental disorders.

During PPI testing a weak pre-stimulus inhibits the response to a subsequent startling stimulus (Swerdlow, 2013). The pre-stimulus acts as a preparatory signal which should normally reduce the startle reaction in the subject; however, in subjects with PPI deficiencies less reduction in startle reaction is observed following the preparatory signal.

Patients with TD and/or OCD are known to have prepulse inhibition (PPI) deficiencies. *Hdc* knockout mice, a model for TD, have PPI deficits. Furthermore, members of an extended family with a deleterious mutation in the *Hdc* gene segregating with affected individuals also display PPI deficiency (Castellan Baldan et al., 2014). Therefore, we wanted to determine if any PPI deficiencies occurred in heterozygous (+/-), knockout mice, heterozygous and/or homozygous *Pnkd*c.415C>T mice.

No significant differences between wild-type, heterozygous or homozygous *Pnkd* knockout out animals were observed (Figure 13a, two-way repeated measure ANOVA $F(2,52)$ $p=0.1170$). This data indicated that knockout of the Pnkd-medium and -long isoform does not affect sensorimotor gating in mice.

We also observed no significant differences between wild-type, heterozygous or homozygous c.415C>T mice (Figure 13b, Two-way repeated measure ANOVA $F(2, 52)$ $p=0.175$). Startle amplitude was also not significantly different between genotypes.

These data show that neither knockout of *Pnkd* gene nor the *Pnkd* c.415C>T nonsense mutation influence sensorimotor gating in mice.

Figure 13: Prepulse Inhibition results for both groups (wild-type, heterozygous and homozygous knockout) and (wild-type, heterozygous and homozygous c.415C>T) mice:

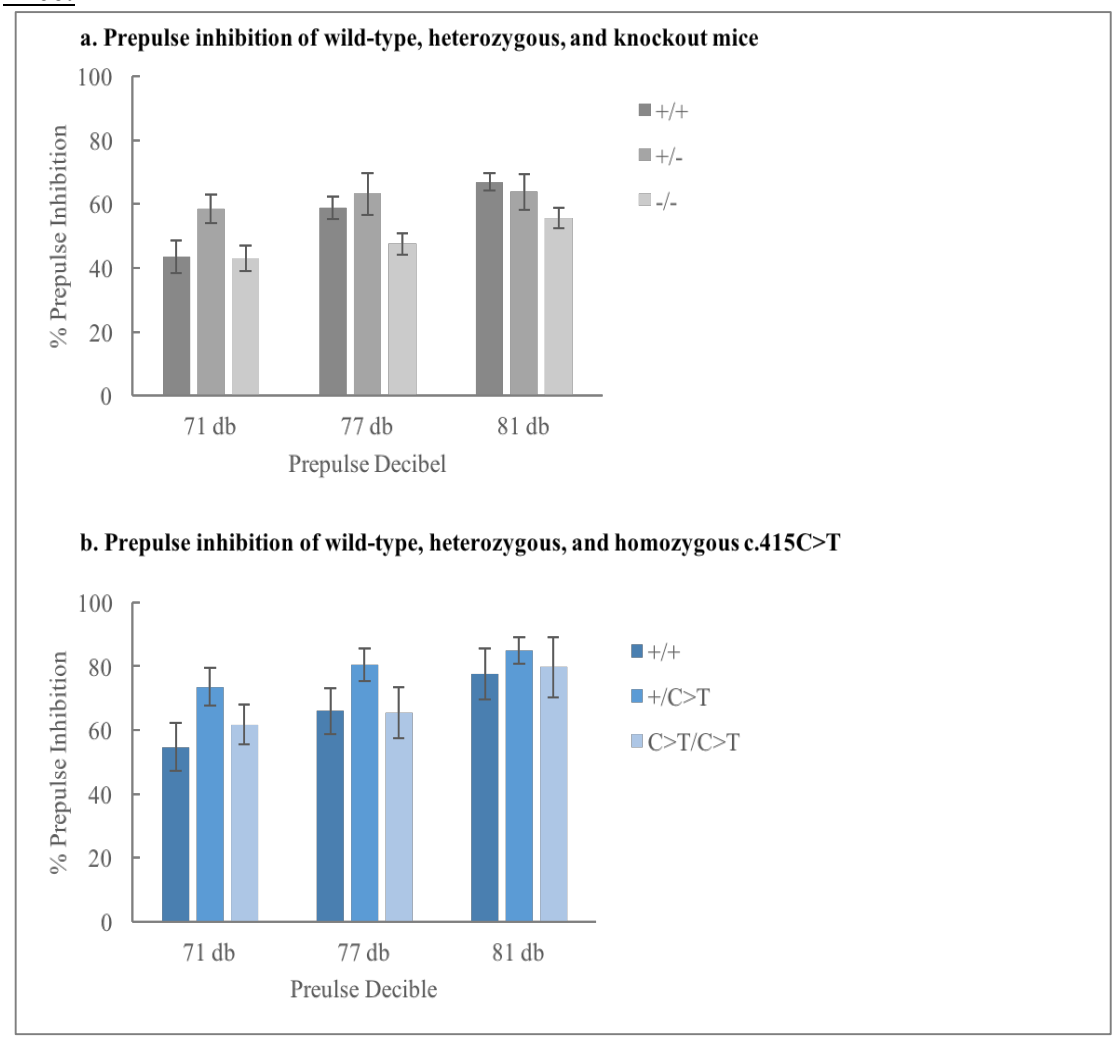

Figure 13: (a) Prepulse inhibition was not significantly different between *Pnkd*$^{+/+}$, *Pnkd*$^{+/-}$, and *Pnkd*$^{-/-}$ genotypes (Two-way repeated measures ANOVA F(2,52) p=0.12) +/+ n=17,+/- n=19, -/- n=19, **dark gray=+/+, medium gray=+/- and light gray=-/-** (b) Prepulse inhibition was not significantly different between *Pnkd*$^{+/+}$, *Pnkd*$^{+/c.415C>T}$, and *Pnkd*$^{c.415C>T/c.415C>T}$ genotypes (Two-way repeated measures ANOVA F(2,52) p=0.18) +/+ n=17, +/C>T n=19, C>T/C>T n=19, **dark blue=+/+, medium blue=+/C>T, and light blue=C>T/C>T**

The results from all of the behavior paradigms performed are summarized in Table 14.

Table 14: Summary of behavior results:

Behavior Paradigm	Group One (*Pnkd*$^{+/+}$, *Pnkd*$^{+/-}$, and *Pnkd*$^{-/-}$)	Group Two (*Pnkd*$^{+/+}$, *Pnkd*$^{+/c.415C>T}$, and *Pnkd*$^{c.415C>T/c.415C>T}$)
Open Field Arena	Knockout mice moved significantly less distance in the first five minutes of the test in comparison to wild-type mice and spent less time in the center of the arena in comparison to heterozygous but only trended less in comparison to wild-type mice	Heterozygous c.415C>T mice spent reduced proportion of time in the center of the arena
Elevated Plus Maze	No significant difference, although Knockout mice had a trend of spending more time in the open arms	Homozygous mutant mice spent proportionately more time in the open arm in comparison to wild-type and heterozygous mutant mice
Marble Burying	Knockout mice buried significantly more marbles then wild-type or heterozygous mice	No significant differences found between genotypes
Prepulse Inhibition	No significant difference found between genotypes	No significant differences found between genotypes

It appears from these results that knockout of the *Pnkd* gene and the nonsense mutation (c.415C>T) of the *Pnkd* at result in distinct behavioral phenotypes, to be discussed in the next section.

1.4 Discussion

Our aim was to determine if either knockout of the *Pnkd* gene or a nonsense mutation at *Pnkdc.*415C>T result in aberrant behavioral phenotypes in paradigms relevant to TD and other related disorders (Table 2). While other mouse models of TD

have been previously studied, this study is unique in that mice were created with a specific SNV found segregating with TD in a three-generation pedigree. We performed behavioral paradigms which are relevant to TD and related disorders. In NIMH's RDoc these behavior paradigms fit into units of analyses for negative valence systems, positive valence systems, and cognitive systems (Tables 1 and 2). The results suggest that homozygous *Pnkd* knockout mice, heterozygous *Pnkd*c.415C>T and homozygous *Pnkd*c.415C>T mice have unique behavioral phenotypes. Upon initial introduction, homozygous *Pnkd* knockout mice had reduced exploration of the open field arena when directly compared to heterozygous (+/-) and wild-type mice (Figure 3). Homozygous knockout mice also had a lower number of rearing bouts; although, the time spent rearing was not significantly different (Figure 4). Additionally, homozygous knockout mice spent a lower proportion of their time in the center of the arena compared to heterozygous (+/-) mice and trended lower in comparison to wild-type mice. (Figure 7). These results indicate there may be a heightened level of fear or "anxiety-like" behavior causing them to explore less.

The results in the open field arena of *Pnkd*c.415C>T mice also hinted at a role for the *Pnkd* gene in "anxiety-like" behavior in mice. Heterozygous *Pnkd*c.415C>T mice spent less time in the center of the arena, indicating an increased level of "anxiety-like" behavior (Figure 8). Interestingly, this effect was not observed in homozygous c.415C>T mice which tracked with wild-type mice in this parameter suggesting that there may be a difference in phenotype between mice with a complete knockout of both the Pnkd medium and long isoform and those which harbor the *Pnkd*c.415C>T SNV.

In the EPM, homozygous *Pnkd* knockout mice had a trend of spending more time in the open arms, although these data were not significant (Figure 9). Homozygous *Pnkdc.415C>T* spent a significantly increased proportion of time in the open arm in comparison to wild-type (Figure 10). These results implicate a role for *Pnkd* in exploration as well as risk assessment. ADHD mouse models have been found to spend more time in the open arms of the EPM (Avale et al., 2004; Zimmermann et al., 2015). ADHD is frequently comorbid with TD and two of the family members heterozygous for the *Pnkd*c.415C>T SNV were diagnosed with ADHD at the time of this study. Therefore, it would not be surprising to find changes in behavior compared to wild-type in mice harboring the same mutation. A lack of phenotypic overlap between homozygous *Pnkd* knockout mice and mice harboring the *Pnkd*c.415C>T SNV was observed in both the OFA and the EPM and the two groups of mice were also distinct in the Marble Burying Task. Homozygous *Pnkd* knockout mice buried significantly more marbles in comparison to wild-type mice (Figure 10) while neither heterozygous *Pnkd*c.415C>T mice nor homozygous *Pnkd*c.415C>T mice had any significant differences in comparison to wild-type or to each other (Figure 11).

From these data and data from the OFA and the EPM, it appears that *Pnkd* knockout mice and mice harboring the *Pnkd*c.415C>T SNV may exhibit different behavioral phenotypes. Together, both groups of mice indicate a role for *Pnkd* in RDoc domains of negative and positive valence systems as well as cognitive systems (Table 1). However, the molecular etiology of the disparate phenotypes between the *Pnkd* knockout and the *Pnkd*c.415C>T SNV warrant further investigation.

As is commonly observed in subjects with TD, some members of the multiplex family heterozygous for the *PNKD*c.415C>T SNV, have TD comorbid with OCD and/or ADHD. Subjects 5001 and 5002 are diagnosed with both TD and OCD. Subject 5004 is diagnosed with chronic tics and ADHD. Subject 5003 is diagnosed with TD, OCD and ADHD. The presence of these comorbid conditions may make it challenging to parse out which symptoms in the human family may be related to *PNKD.*

One major limitation of this study is that, due to timing constraints, group one ($Pnkd^{+/+}$, $Pnkd^{+/-}$, and $Pnkd^{-/-}$) was tested more than a year prior to group two ($Pnkd^{+/+}$, $Pnkd^{+/c.415C>T}$, and $Pnkd^{c.415C>T/c.415C>T}$). However, in each group wild-type mice were used as a control. This may have led to differences between groups overall. In particular, in the open field and marble burying test the first group ($Pnkd^{+/+}$, $Pnkd^{+/-}$, and $Pnkd^{-/-}$) tested were more active, even among wild-type animals. However, it remains possible that the nonsense mutation *Pnkd*c.415C>T and the knockout of the gene lead to qualitative behavioral differences. In chapter 2, we aimed to further investigate a potential molecular basis for these differences, investigating whether the medium and long Pnkd transcripts with the early protein synthesis termination codon resulting from the C>T transition mutation, undergo equal degrees of degradation.

Chapter 2

THE MEDIUM ISOFORM OF *Pnkd* ESCAPES NONSENSE MEDIATED DECAY THROUGH AN AS YET UNKNOWN MECHANISM

2.1 Introduction

Since *Pnkd* heterozygous and homozygous mutant mice appear to have unique behavioral phenotypes, we wanted to explore a potential molecular basis for these

differences. As noted previously, the *Pnkd* gene has multiple isoforms generated from alternative mRNA splicing (Figure 1). The *Pnkd*c.415C>T SNV (nonsense mutation) discovered in the TD multiplex family reported in this study results in an early protein synthesis termination codon in both the medium and long isoform but no changes in the short isoform. The long and medium isoform share the same C-terminal sequence (the last 8 exons of each transcript). However, the N-terminal sequences are different between the two isoforms. While the long isoform shares a promoter and the first two exons with the short isoform, the medium isoform has a unique N-terminal exon and promoter. Because the *PNKD*c.415C>T mutation results in an early termination codon in both the medium and long isoforms of Pnkd in both mice and humans we anticipated that both transcripts would be subject to nonsense mediated decay (NMD).

NMD acts as both a maintenance and protective mechanism within the cell, regulating the steady state levels of normal mRNA transcripts while also degrading aberrant transcripts with early termination codons, thereby preventing translation into dysfunctional or nonfunctional proteins. NMD requires the replacement of the exon junction protein complex with a translation termination protein complex (Lindeboom et al., 2016).

Previously, we reported that human neurons derived from iPSC of individuals heterozygous for the PNKDc.415C>T, had reduced levels of the PNKD-long transcript as well as RIM1. A reduction in RIM1 protein concentration was not surprising, as it was shown by Ptacek et al., 2014 that, in comparison to wild-type mice, homozygous *Pnkd* knockout mice had reduced levels of RIM1 in synaptic isolates from the mouse frontal cortex. Additionally, PNKD protein was found to stabilize RIM1 protein at the

presynaptic terminal in mouse cortical neurons (Shen et al., 2015). Because of the critical role that RIM1 plays in Ca^{2+} -induced neurotransmission and the reduction of RIM1 in subjects heterozygous for the *Pnkd*c.415C>T SNV, we originally proposed that the TD observed within the extended pedigree under study was likely due to the haploinsufficiency of the PNKD-long isoform that resulted in reduction of RIM1 protein in these individuals, thus altering synaptic transmission (Sun et al., 2017).

Surprisingly, my qPCR studies of cDNA generated from the RNA of mouse brain sections (cortex, cerebellum, and striatum) of homozygous *Pnkd*c.415C>T mice show that while the mutant Pnkd-long isoform is nearly obliterated in homozygous *Pnkd*c.415C>T mice, the mutant Pnkd-medium transcript appears relatively stable. This indicates that the truncated medium transcript somehow avoids rapid degradation. This could potentially lead to a truncated Pnkd medium protein isoform that could theoretically interfere with the wild-type protein or perhaps gain a new function. Therefore, it is possible that the mutant medium isoform is the cause of the TD phenotype within the pedigree studied. Another possibility is that reduction in the long isoform due to NMD of the transcript harboring the early termination codon and the presence of an aberrantly expressed medium isoform both are etiological factors.

In human neurons derived from iPSC of subjects heterozygous for the *PNKD*c.415C>T SNV,PNKD–medium mRNA transcript expression levels are not significantly reduced while PNKD–long mRNA transcript levels are (personal communication, Nawei Sun). In this chapter I report that the Pnkd-long mRNA transcript harboring the *Pnkd*c.415C>T is rapidly degraded while mutant -medium

mRNA transcript appears stable despite harboring the same early termination codon and having the same c-terminal sequence as the long isoform.

2.2 Materials and Methods

2.2.1 Isolation of RNA from tissue Mouse brain (Cortex, Striatum, and Cerebellum) and liver were dissected over ice in RNAse free PBS. Directly following dissection tissue was placed in RNAlater (Sigma Aldrich) and incubated in 4°C overnight. The next day, trizol was used to isolate RNA. RNAlater was removed from tissue samples. 200 ml of Trizol was then added to each tube. Tissue was homogenized using a homogenization gun. Following homogenization, an additional 800 ml of Trizol was added and the samples were mixed by gentle pipetting. After a 10 minute incubation period on ice, 200 ml of chloroform was added and shaken vigorously for 20-30 seconds. The samples were then incubated on ice for an additional 30 minutes. The aqueous and organic layers were separated through centrifugation at 12000Xg for 15 minutes in 4°C. The aqueous layer was removed to a new tube and mixed with 500 ml of 100% isopropanol by inverting each tube 15X. Samples were incubated for 1 hour to overnight in -20°C. After incubation, RNA was pelleted through centrifugation at 12000XG for 30 minutes in 4°C. Samples were washed in 70% ethanol for and spun for 5 minutes at 12000XG. The pellet was suspended in 44 µl of RNAse free water and incubated for 10 minutes at 60°C with vortexing every 2.5 minutes.

Contaminating DNA was removed using DNA free kit (Ambion): One µl of DNAse and five µl of 10X DNAse I buffer solution to each sample. Samples were next incubated 37°C for 30 minutes. Following which 5 µl of DNAse inactivation solution was added to each sample and incubated 3 minutes at room temperature. Samples were

spun for 1.5 minutes at 2000 RPM in 4°C. The top layer containing the RNA was removed. The final concentration of RNA was determined using a nanodrop spectrophotometer (ThermoFisher).

2.2.2 Synthesis of complementary DNA (cDNA) cDNA was synthesized using the Applied Biosystems High Capacity cDNA synthesis kit. The PCR formula is listed in the table below (Table 15).

Table 15: cDNA synthesis reaction mixture:

	Amount
10X RT Buffer	10 µl
25X dNTP mixture (100 mM)	8 µl
Random Primers	10 µl
Oligo dT	10 µl
Reverse Transcriptase	5 µl
RNAse inhibitor	10 µl
RNA	1 µg
Water	to 100 µl

The cDNA thermo cycling conditions synthesis conditions are in the table below (Table 16).

Table 16: cDNA synthesis thermo cycling conditions:

	Step 1	Step 2	Step 3
Temperature	25°C	37°C	85°C
Time	10 minutes	75 minutes	5 minutes

2.2.3 Semi-quantitative qPCR The standard curve method was used to determine mRNA transcript levels of the three known Pnkd isoforms (short, medium, and long). Beta-actin was used as a housekeeping gene control for all experiments. A unique primer pair specific to each isoform was used to differentiate expression levels of the long, medium and short isoform. The sequence for the three primer pairs for Pnkd short, medium, and long isoforms as well as the primer pair for the mouse beta-actin transcript is listed in the table below. All primers were designed to straddle exon-exon junctions (Table 17).

Table 17: Primer pairs for semi-quantitative qPCR experiments:

Transcript Name	5'->3' Sequence
Pnkd Short Forward	GAGCTAGAATACATTCCCAG
Pnkd Short Reverse	TTCCACTTCCTGCTTGGTGA
Pnkd Medium Forward	CTATTCTTCGCCTTCGTGCT
Pnkd Medium Reverse	GGATGGGAAGCACCTTCACT
Pnkd Long Forward	CCCTCTCCCCTGAGCTAGAA
Pnkd Long Reverse	GAGAGGACAGGGATCGGAAG
Beta-Actin Forward	CTGTCCCTGTATGCCTCTG
Beta-Actin Reverse	ATGTCACGCACGATTTCC

A standard curve was generated for each primer using wild-type cDNA from the same tissue type. Standard curves had 6 points each with a 1:4 dilution (256X, 64X,

16X, 4X, 1X, Non template control). To generate the standard curve 6 µl of wild-type cDNA was added to 18 µl of water.

2.2.4 Determination if exon skipping occurs in the mRNA of the mutated *Pnkd* gene

An endpoint PCR amplification reaction on cDNA was done to determine if exon skipping occurs in the mutated *Pnkd* locus allowing the medium isoform to escape nonsense mediated decay. The CRISPR/CAS9 generated mutation occurs in exon 6 of the mouse *Pnkd* gene. Because the mutation affects both the long and medium isoform, primers were created which would uniquely amplify cDNA generated from specifically from either the long or medium mRNA. Below is a table of primers used for these reactions (Table 18).

Table 18: Primers for exon skipping

Primer Name	5'->3' sequence
PnkdExon4-Forward	ATGACGCGCAGCCAGCGGCT
PnkdExon5-Forward	CAAAGGCCACTCCAAAACTC
PnkdExon6-Forward	GCTTCCCATCCCTGTCCTCT
PnkdExon6-Reverse	GCACAGCCCTCGGGTCTGA
PnkdExon7-Reverse	TGCAGAGAATGGCAACCAGT

Long isoform PCR amplifications were done with primers which amplified the region between exon 2 and exon 6 and between exon 2 and exon 7. Medium isoform PCR amplifications were done with primers which amplified the region between exon 4 and 6 and between exon 4 and exon 7.

2.3 Results

qPCR of *Pnkd* transcripts In order to investigate if either or both of the Pnkd-medium or -long transcripts harboring the *Pnkd*c.415C>T are rapidly degraded, qPCR of cDNA generated from mRNA from the prefrontal cortex, striatum, and cortex was completed. Additionally, tissue samples from the liver were analyzed to confirm that the expression of the long isoform outside of the nervous system is below the limit of detection by qPCR. Additionally, the liver has high expression of Pnkd-medium isoform (Lee et al., 2004).

The specificity of the primers designed to exclusively amplify Pnkd -short, -medium, and -long mRNA transcripts were confirmed through isolation of mRNA from forebrain tissue of all three genotypes followed by RT-PCR and qPCR analysis. The correct product size and specificity for each primer was confirmed by size analysis on Agarose gel electrophoresis. The PCR products were also sequenced as further confirmation. Transcript expression levels were analyzed using qPCR analysis (Figure 14).

Figure 14: qPCR of *Pnkd* cDNA transcripts following RT-PCR in the forebrain of wild-type, heterozygous and knockout mice:

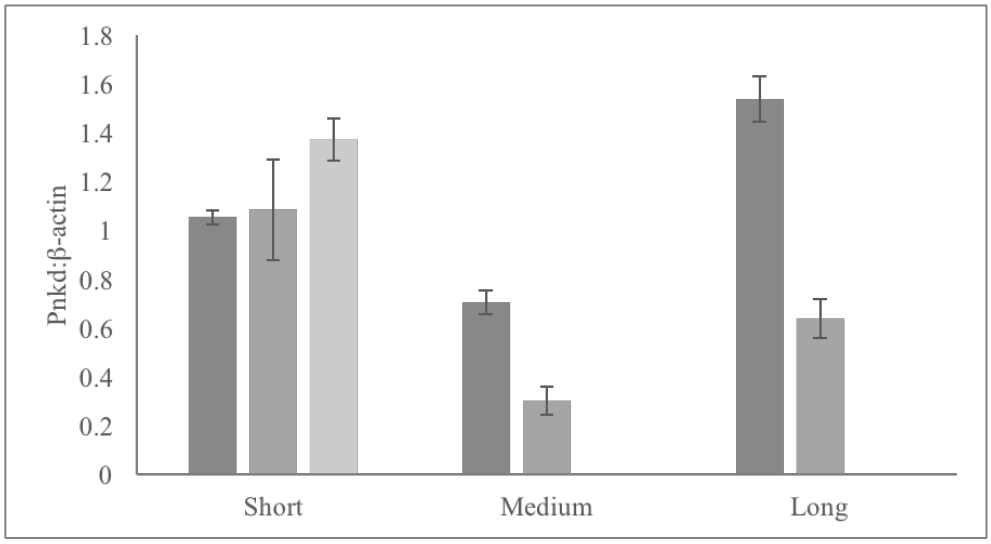

Figure 14: The short transcript's expression levels were not significantly different between the three genotypes. In heterozygous mice the total medium and long isoform are reduced by 58% and 59%, respectively, and both transcripts are completely abolished in the knockout mice as expected. +/+ n=3, +/- n=3, and -/- n=3. **Dark gray=+/+, Medium Gray=+/-, and Light Gray=-/-**

As noted previously, *Pnkd* knockout mice maintain the exonic sequence to synthesize the short isoform transcript while exons affecting the medium and long isoforms are replaced by a *neo*^{r} cassette. Given these facts, we expected the mRNA transcript levels of the short isoform would not be significantly different between *Pnkd* wild-type, heterozygous and homozygous knockout mice. It was also anticipated that *Pnkd* heterozygous mice would have roughly one-half of transcript level of *Pnkd* wild-type mice and that homozygous *Pnkd* knockout would have no measurable mRNA transcript of both the medium and long isoforms. As expected the amount of the short isoform mRNA transcript did not differ significantly between the three genotypes (One-way ANOVA F (2,6) p=0.279). *Pnkd* heterozygous mice transcript levels of the

medium and long isoforms were reduced by 58% and 59%, respectively. Homozygous *Pnkd* knockout mice had undetectable levels of both the medium and long isoform. These experiments proved that the primers designed to amplify only the short, medium, and long isoform are specific. Additionally, the qPCR experiments show that absence of the long or medium isoform in forebrain tissue does not result in isoform compensation through increased expression of the short isoform in *Pnkd* knockout mice.

We next investigated if the presence of the early termination codon caused by the *Pnkd*c.415C>T resulted in degradation of the medium and long transcripts, or alternatively, if the transcripts persisted. We hypothesized the premature termination codon would result in activation of the NMD pathway leading to rapid degradation of both the medium and long isoform and we would see no significant changes in expression in the short isoform. Tissue was removed from brain regions critically important in executing both voluntary and/or involuntary movement (prefrontal cortex, striatum, and cerebellum). Liver was also isolated as a negative control for the neuronal form.

The prefrontal cortex is important in higher executive cognitive function. In functional MRI studies subjects with more severe tics show more activation in their prefrontal cortex (Eichele and Plessen, 2013). In a volumetric MRI study, grey matter within the PFC was reduced in subjects with TD and no other comorbidity (Müller-Vahl et al., 2009) . The PFC is likely critically important in the suppression of tics (Ganos, 2016). Additionally, the *Pnkd* gene helps regulate neurotransmission at the presynaptic terminal demonstrating a potential etiological link between the manifestation of TD and mutations in the *Pnkd* gene (Lee et al., 2012; Shen et al., 2015).

All three *Pnkd* mRNA isoforms were expressed in the PFC (Figure 15).

Figure 15: qPCR of Pnkd transcripts following RT-PCR of mouse Prefrontal Cortex

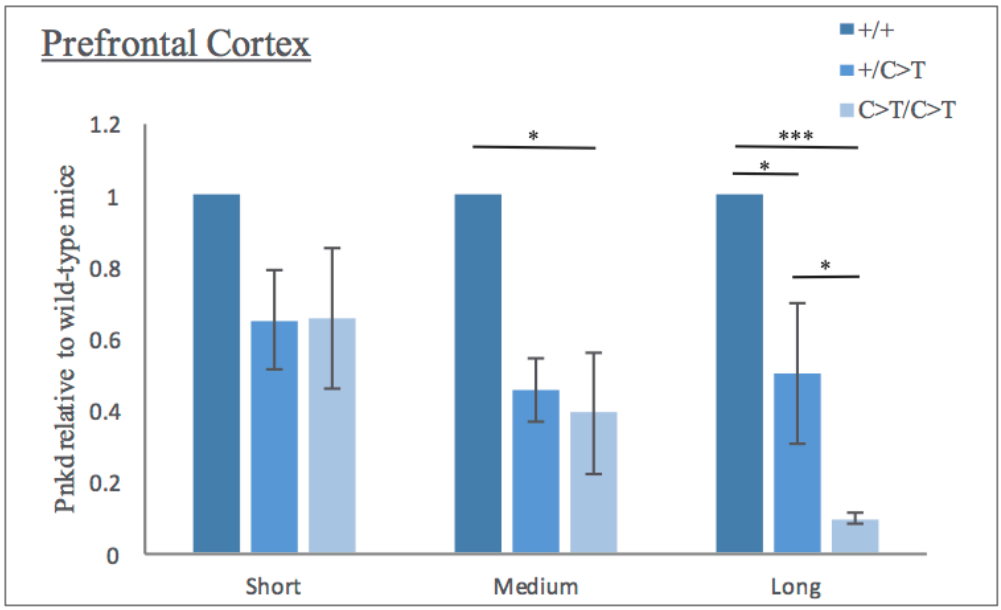

Figure 15: qPCR data of the short, medium and long *Pnkd* mRNA isoforms in the prefrontal cortex of wild-type, heterozygous, and homozygous mutant mice. All samples were first normalized to the housekeeping gene β-actin and the fraction of expression of each isoform in the heterozygous and homozygous mutant mice compared to wild-type mice is displayed here. The short isoform had no significant difference in expression between genotypes. The relative amount of the medium isoform of the homozygous mutant mouse is significantly lower than in wild-type mice but nearly equivalent to heterozygous mutant mice. The relative amounts of the long isoform were significantly different from the wild-type in both heterozygous mutant mice and homozygous mutant mice. +/+ n=4, +/C>T n=3, C>T/C>T n=4. *=$p<0.05$, **=$p<0.001$, ***=$p<0.0001$, in comparison to wild-type, Tukey's multiple comparisons test. **Dark blue=+/+, Medium blue=+/C>T and Light Blue=C>T/C>T**

As predicted, the levels of the short isoform which consists of exons 1-3 and therefore does not contain the termination codon within exon 6 were not significantly different between genotypes (One-Way ANOVA $F(2, 8)$ $p=0.105$). Because the early termination codon in mutated, long and medium transcripts could result in a truncated protein if translated, but we anticipated that mutant transcripts of these mRNA isoforms

would be degraded by nonsense mediated decay. As expected, mutated transcripts of the Pnkd-medium and -long isoforms were significantly different between genotypes in the prefrontal cortex (Figure 15: One-way ANOVA F (2,8) p=0.020 and p=0.0003, respectively). Heterozygous *Pnkd*c.415C>T mice had 46% of wild-type expression levels of the medium isoform transcript, although the difference between wild-type and heterozygous *Pnkd*c.415C>T mice was not statistically significant (Tukey's multiple comparisons p=0.106). Interestingly, homozygous *Pnkd*c.415C>T mice maintained comparable levels of the medium isoform transcript in comparison to heterozygous mice (Tukey's multiple comparisons p=0.631). Although, homozygous mutant mice did have significantly lower levels of the medium transcript in comparison to wild-type mice (Tukey's multiple comparisons p=0.018); they still maintained 39% of wild-type expression levels.

In stark comparison to this, expression of the long transcript in homozygous *Pnkd*c.415C>T mice remained at only10% expression levels in comparison to wild-type mice (Tukey's multiple comparisons p=0.002). Heterozygous *Pnkd*c.415C>T mice also had significantly lower expression levels of the long transcript in comparison to wild-type mice (Tukey's multiple comparisons, p=0.014). Expression of the long isoform remained at 50% in heterozygous *Pnkd*c.415C>T mice.

Therefore, it appears that in the PFC, unlike the mutant long transcripts which appears to be efficiently degraded, mutant medium transcripts appear to evade full or efficient degradation.

We next investigated if the same phenomena could be observed in the striatum. As mentioned previously, the basal ganglia, which includes the striatum has been widely

implicated in playing a critical role in the etiology of TD. The striatum is part of the CSTC loop which regulates both involuntary and voluntary movement. Aberrations in the basal ganglia have been found in subjects with TD (Obeso et al., 2014). As expected there was no significant difference between the short isoform of the three genotypes (One-way ANOVA F (2,8) p=0.184). A significant difference in expression of the medium transcript between the three genotypes (One-way ANOVA F (2,8) p=0.008). Both the heterozygous *Pnkd*c.415C>T (Tukey's multiple comparisons p=0.0038) and the homozygous *Pnkd*c.415C>T (Tukey's multiple comparisons p=0.0009) had significantly lower expression levels then wild-type mice. However, in comparison to each other heterozygous and homozygous *Pnkd*c.415C>T mice were not significantly different from each other (Tukey's multiple comparisons p=0.751). The expression of the medium isoform in heterozygous and homozygous *Pnkd*c.415C>T mice remained at 42% and at 32% of that of wild-type mice, respectively (Figure 16).

Figure 16: qPCR of Pnkd transcripts following RT-PCR of mouse Striatal RNA

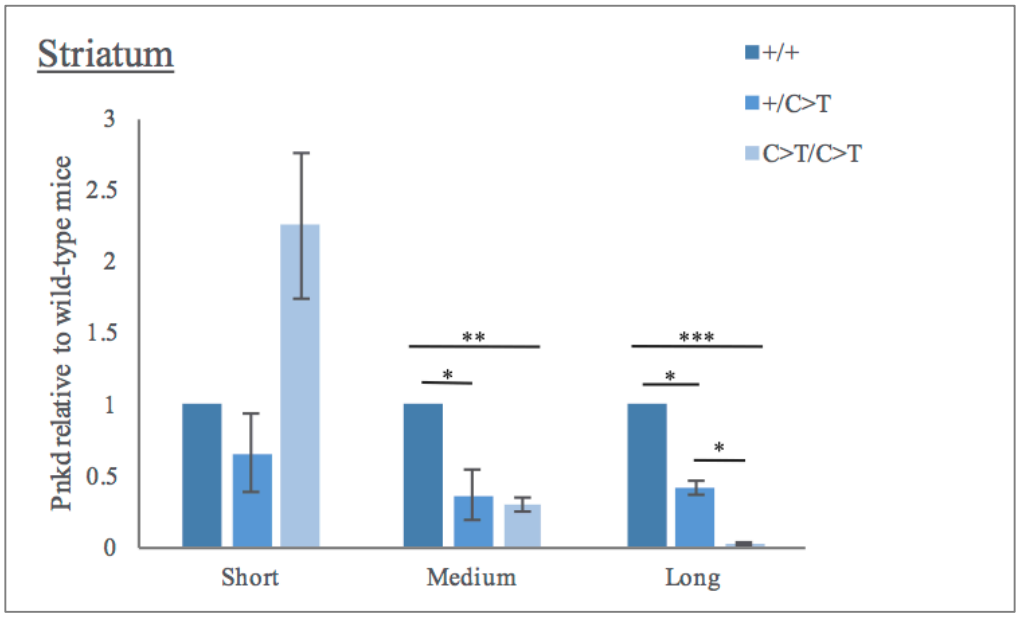

Figure 16: qPCR data of the short, medium, and long Pnkd isoforms in the striatum of wild-type, heterozygous, and homozygous mutant mice normalized to wild-type mice. No significant changes in expression in the short were observed between genotypes. Heterozygous and homozygous c.415C>T mice had similar expression levels of the medium transcript to one another, but both were significantly lower than wild-type. The long isoform was nearly completely absent in homozygous c.415C>T mice and heterozygous c.415C>T mice had an expression level in between that of wild-type had homozygous mutant mice. +/+ n=4, +/C>T n=3, C>T/C>T n=4. *=$p<0.05$, **=$p<0.001$, ***=$p<0.0001$, in comparison to wild-type, Tukey's multiple comparisons test. **Dark blue=+/+, Medium blue=+/C>T and Light Blue=C>T/C>T**

As we observed in the PFC, the mutant long isoform underwent near complete degradation in the striatum. The three genotypes differed significantly from one another (One-way ANOVA F (2,8) $p<0.0001$). Heterozygous mutant mice maintained 42% long transcript expression levels in comparison to wild-type. Heterozygous *Pnkd*c.415C>T mice had significantly lower expression levels of the long transcript in comparison to wild-type mice (Tukey's Multiple Comparisons Test, $p=0.0027$). Homozygous *Pnkd*c.415C>T mice maintained only 3% of the long transcript expression level observed in wild-type mice. Homozygous *Pnkd*c.415C>T mice had significantly

lower expression of the long transcript in comparison to both wild-type and heterozygous *Pnkd*c.415C>T mice (Tukey's Multiple Comparisons, $p<0.0001$ and $p=0.023$, respectively). Therefore, it appears that in the striatum, as in the PFC, the medium RNA transcript avoids full degradation by cellular machinery while the long isoform is rapidly degraded.

The transcript levels of the three Pnkd isoforms were next examined in the cerebellum. The cerebellum is a hindbrain region important in the refinement of learned motor behaviors, movement reaction timing, and balance control. It remains unclear if aberrations in the cerebellum have an etiological role in TD. In 2014, it was discovered that the cerebellum and basal ganglia can directly and rapidly communicate. Over-activation of this disynaptic pathway was found to be the cause of a mouse model with cerebellar induced dystonia, an involuntary movement disorder (Chen et al., 2015). It's possible, that at least some subjects with TD, have changes in the cerebellum which cause aberrations in the communication between the structures of the basal ganglia and the cerebellum causing tics. Although, one study of 20 male subjects with TD found no gross volume changes in the cerebellum in comparison to unaffected individuals, another study of over 150 subjects with TD found the volumes of gray matter in the cerebellum significantly changed in subjects with TD. Severity of tics correlated with smaller size. Intriguingly, males had lower cerebellar gray matter volume within the cerebellum compared to females regardless of diagnosis providing a potential explanation for the male bias within TD diagnosis (Müller-Vahl et al., 2009; Tobe et al., 2010). Due to the functional role of the cerebellum in movement control as well as

recent evidence of a direct communication link between the cerebellum and the striatum, we wanted to investigate the expression of *Pnkd* in this tissue type.

We anticipated the same pattern of expression observed in the prefrontal cortex and the striatum. The short isoform transcript would be unchanged between the three genotypes, the medium transcript harboring the c.415C>T SNV would be relatively stable, and the long mutant transcript would be mostly degraded. As expected, no significant difference was found in expression levels of the short isoform between genotypes, although it neared significance (Figure 17, One-way ANOVA F (2,8) p=0.053) and might warrant further investigation in the future involving more samples. The expression levels of the medium transcript in all genotypes neared equivalence (Figure 17, One-way ANOVA F (2,8) p=0.945). It was surprising to find little to no reduction in expression of the medium transcript in either the heterozygous or homozygous *Pnkd*c.415C>T mice. Heterozygous and homozygous *Pnkd*c.415C>T mice each maintained greater than 90% of the expression level of the *Pnkd* medium transcript found in wild-type mice (Figure 17).

Figure 17: qPCR of *Pnkd* transcripts following RT-PCR of mouse cerebellum RNA

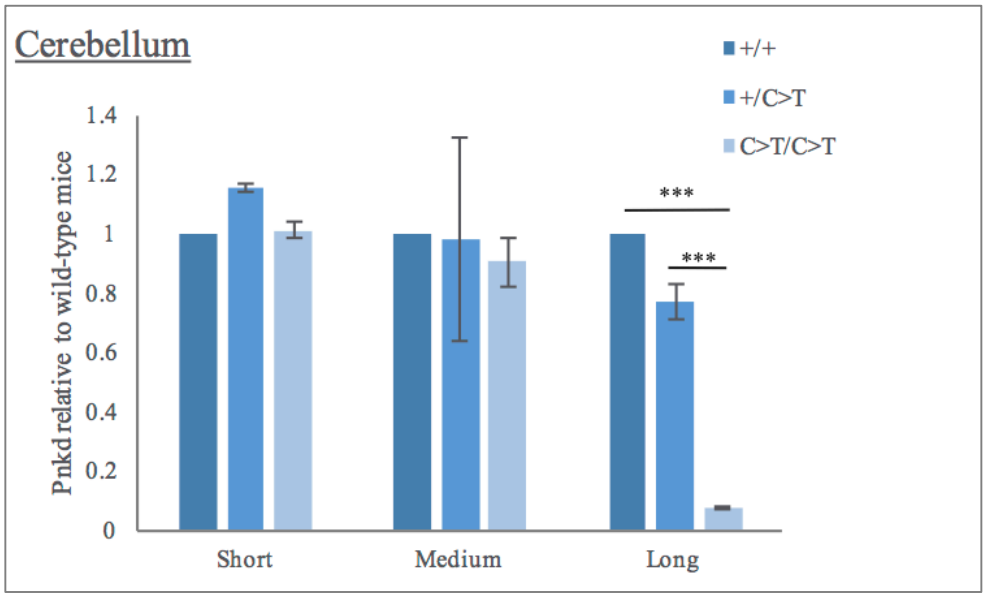

Figure 17: qPCR data of the short, medium, and long Pnkd isoforms in the cerebellar of wild-type, heterozygous, and homozygous mutant mice. No significant differences between genotypes was observed in the expression levels of the short or medium isoforms. The long isoform had no significant difference in expression levels between the wild-type and heterozygous mutant mice. Homozygous mutant mice had significantly reduced levels of the long isoform in comparison to both wild-type and heterozygous mutant mice. +/+ n=4, +/C>T n=3, C>T/C>T n=4. ***=p≤0.0001, in comparison to wild-type, Tukey's multiple comparisons test. **Dark blue=+/+, Medium blue=+/C>T and Light Blue=C>T/C>T**

Similar to the observations of expression levels of the long transcript in the prefrontal cortex and the striatum the long transcript's expression level was significantly different between genotypes (Figure 17, One-way ANOVA F (2,8) $p<0.0001$). Again expression levels of the long transcript were significantly diminished in homozygous *Pnkd*c.415C>T mice (Tukey's Multiple Comparisons, $p<0.0001$). Expression of the long transcript remained at 7% of the expression levels in wild-type mice. A significant reduction in expression of the Pnkd long isoform was also observed in homozygous *Pnkd*c.415C>T mice in comparison to heterozygous *Pnkd*c.415C>T

mice (Tukey's multiple comparisons $p<0.0001$). Although reduced, there was no significant difference in the expression levels of the Pnkd long transcript in heterozygous *Pnkd*c.415C>T mice in comparison to wild-type mice (Tukey's multiple comparisons $p=0.069$). Expression levels remained at 76% that of wild-type mice in heterozygous *Pnkd*c.415C>T mice. Additionally, homozygous *Pnkd*c.415C>T mice had significantly lower levels of expression of the long transcript in comparison to that of heterozygous *Pnkd*c.415C>T mice (Tukey's multiple comparisons $p=0.0001$). (Figure 15).

To determine if medium mutant transcript would be detectable in heterozygous mice we performed endpoint RT-PCR on wild-type, heterozygous and homozygous *Pnkd*c.415C>T mice on whole mouse brain tissue and sequenced purified cDNA products. Sequencing revealed detectable levels of *Pnkd*c.415C>T medium isoform, but no detectable levels of *Pnkd*c.415C>T long isoform in heterozygous mice (Figure 18).

Figure 18: Sequencing of purified cDNA products from wild-type, heterozygous and homozygous *Pnkd*c.415C>T mice

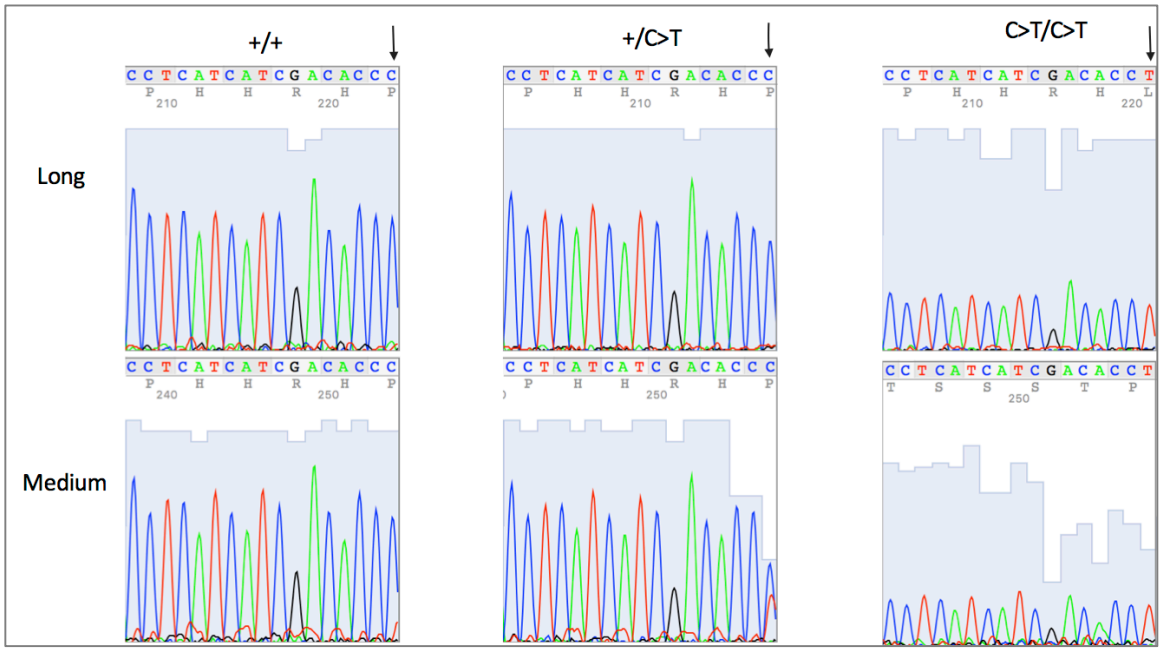

Figure 18: The mutant form of the medium isoform is detectable in the cDNA of heterozygous *Pnkd*c.415C>T mice while the long is not indicated inefficient degradation of the medium c.415C>T isoform. The black arrow indicates the site of the C>T transition in the *Pnkd* gene

In summary, in homozygous *Pnkd*c.415C>T mice resulting in an early termination codon within exon 6 of the *Pnkd* gene, the mutated form of the medium transcript appears not to be fully or efficiently degraded in the prefrontal cortex, striatum, or cerebellum while the mutated long transcript which contains the same early termination codon appears to be rapidly degraded in these brain tissue regions.

Next we wanted to investigate if incomplete degradation of the medium isoform harboring the *Pnkd*c.415C>T SNV would also be apparent in a non-neuronal tissue type. The *Pnkd* medium isoform is highly expressed in the liver; therefore we studied

this tissue type (Lee et al., 2004). The long isoform is not expressed outside of the nervous system and indeed, we found no expression of neither wild-type nor mutant long form in the liver of any genotype (data not shown). In comparison to brain tissue, the *Pnkd* medium transcript was expressed at almost 4-fold greater levels in the liver compared to the brain of wild-type mice (Figure 19, unpaired t-test, p=0.0016). In the brain where expression of the medium isoform was lower then found in the liver, there was a significant difference in expression between genotypes (Figure 19, One-way ANOVA, F (2,10), p=0.0059). Both heterozygous and homozygous *Pnkd*c.415C>T mice had significantly lower expression levels the *Pnkd* medium transcript in comparison to wild-type (Tukey's multiple comparisons test, p=0.032 and 0.0047, respectively). Heterozygous *Pnkd*c.415C>T mice maintained 62% of expression of the *Pnkd* medium transcript levels found in wild-type mice. Homozygous *Pnkd*c.415C>T mice maintained 47% of the expression of *Pnkd* medium transcript found in wild-type mice, and did not differ significantly from heterozygous *Pnkd*c.415C>T mice in the brain. These results corroborate with our observations in the prefrontal cortex, striatum, and cerebellum that the Pnkd medium transcript is stable or at least not rapidly degraded. In the liver, heterozygous mutant mice maintained nearly equivalent levels of the Pnkd medium transcript in comparison to wild-type (Figure, 19, Tukey's multiple comparisons test, p=0.99). However, levels of the Pnkd medium transcript in homozygous *Pnkd*c.415C>T mice was significantly reduced in comparison to both wild-type and heterozygous *Pnkd*c.415C>T mice (Figure 19, Tukey's multiple comparisons test, p=0.013 and 0.009, respectively). In the liver, the expression level of

the *Pnkd* medium transcript in homozygous *Pnkd*c.415C>T mice remained at 14% of that found in wild-type (Figure 19).

Figure 19: Comparison of expression of the *Pnkd* medium transcript in Mouse brain and liver

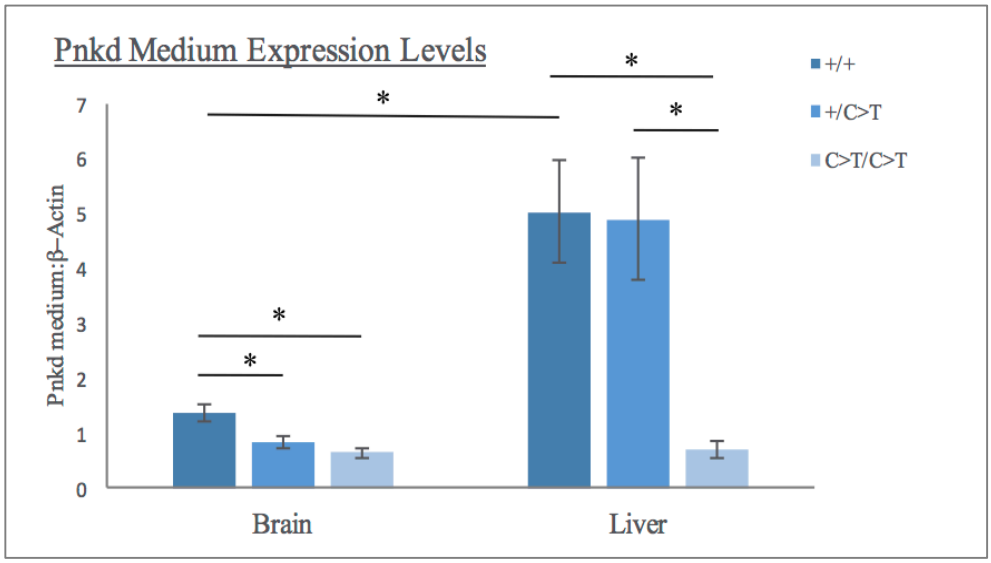

Figure 19: The expression level of the *Pnkd* medium isoform is significantly lower in the brain in comparison to the liver. Heterozygous and homozygous mutant mice had significantly lower levels of expression of medium isoform in the brain but were not significantly different from each other. In the liver homozygous mutant mice had significantly lower levels of expression of the medium isoform in comparison to both wild-type and heterozygous mice. +/+ n=4, +/C>T n=4, C>T/C>T n=5. *=p<0.05 **Dark blue=+/+, Medium blue=+/C>T and Light Blue=C>T/C>T**

It's unclear from these results if the Pnkd mutant medium transcript maintains stability in the liver. However, homozygous *Pnkd*c.415C>T mice have very little Pnkd medium transcript indicating that perhaps the mechanism protecting this transcript from degradation is restricted to neuronal tissue. Differences in NMD decay efficiencies has been observed in different tissue types so it's possible that the brain does not decay the medium transcript as efficiently as occurs in the liver (Zetoune et al., 2008). However,

the basal expression level is significantly higher in the liver in comparison to the brain (Figure 19). The absolute expression levels of the –medium transcript in the brain and liver of homozygous mutant mice are nearly equivalent making it difficult to determine if there are any tissue specific effects from these results.

Early termination codons have been shown to trigger exon skipping allowing translation of a mutant protein (Liu et al., 2001). The early termination codon in the mutant *PNKD* gene is in exon 6. We wanted to determine if in mutant transcripts any alternatively spliced isoforms were created by skipping of exon 6 in mice harboring the nonsense mutation within exon 6 of the *Pnkd* gene. Primers were designed against flanking exons which would specifically amplify Pnkd-medium between (exons 4 and 7). The PCR products were run on an agarose gel (Figure 20a), purified and sequenced. In both *Pnkd* wild-type and *Pnkd* homozygous mutant mice a specific product of the expected size (310 bp) was amplified (Figure 20). Sequencing revealed no changes in exon to exon junctions between *Pnkd* wild-type and homozygous mutant mice (data not shown).

In addition to exon skipping, read through of early termination codons can also occur (Dabrowski et al., 2015). If read through of the early termination codon in exon 6 of the *Pnkd* gene occurs, we would expect a c-terminal antibody to be able detect a near full-length version of both Pnkd –medium and –long isoforms. We conducted western blotting of mouse brain lysates using a c-terminal antibody (Ptacek et al 2012) and were unable to detect any Pnkd-medium or –long isoform in homozygous mutant mouse brain. Both Pnkd isoforms were detectable in wild-type and heterozygous mutant mice

(Figure 20b). Therefore, its unlikely that the early termination codon within the *Pnkd* gene is bypassed.

Figure 20: No exon skipping occurs in the medium isoform transcript

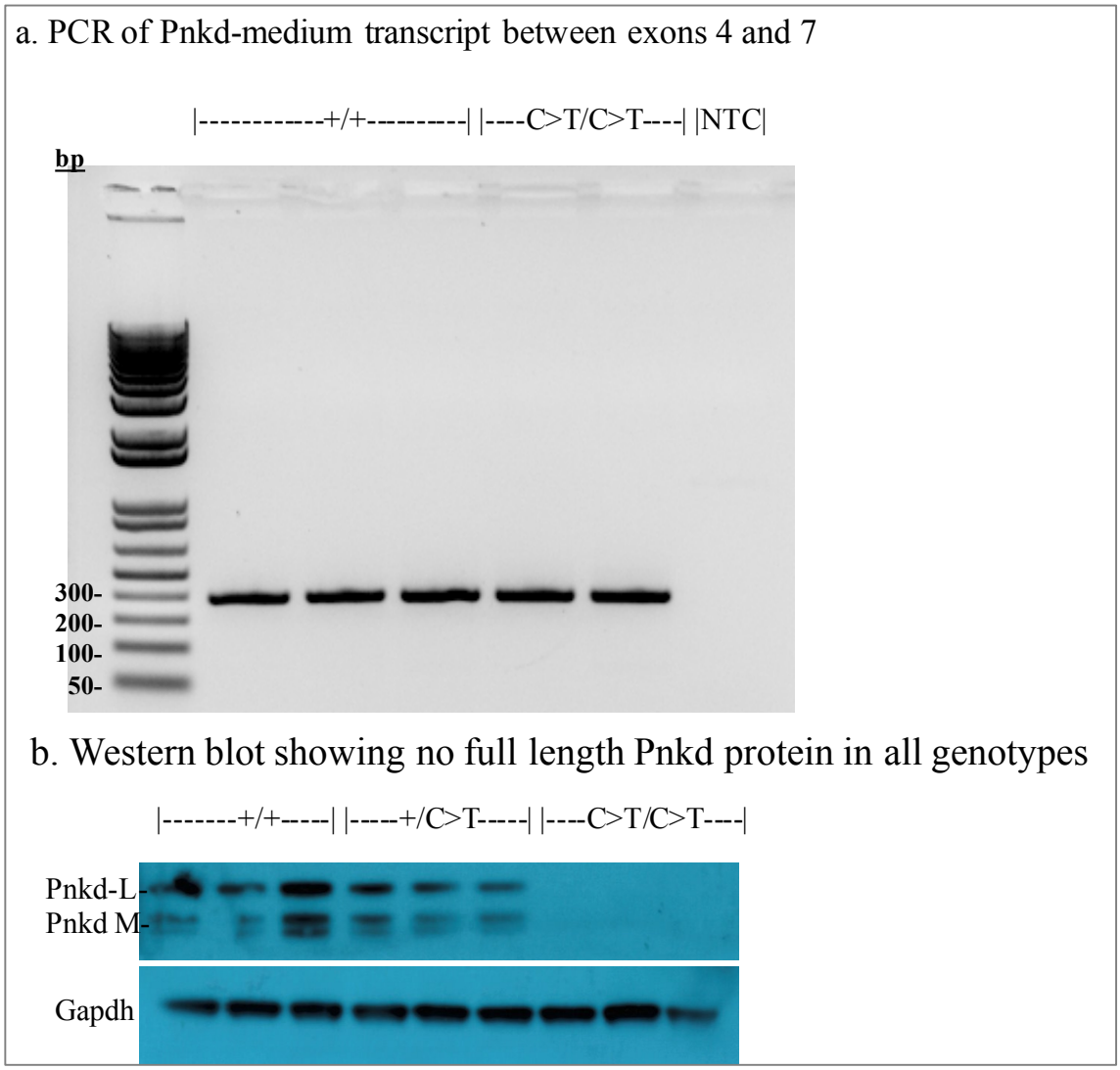

Figure 20: (a) Gel of RT-PCR of both wild-type and homozygous mutant mice showing no skipping of exon 6 in mutant cell (b) Western not using a c-terminal antibody demonstrating read through of the early termination codon does not occur in mouse brain protein lysates

2.4 Discussion

In this chapter, we reported the rapid degradation of the Pnkd-long mRNA transcript and the apparent evasion of NMD by the medium isoform in tissue dissected from the prefrontal cortex, striatum, and cerebellum of mouse brain. Because the medium and long isoform differ only upstream of the *Pnkd*c.417C>T nonsense mutation, it's likely that the difference in stability between the two transcripts is due to differences found in this region. The efficiency of NMD to degrade mutant transcripts with premature termination codons varies considerably between transcripts and is dependent on multiple factors. The distance of a premature termination codon (PTC) to the exon-exon junction is a primary determinant of NMD efficiency. A PTC that is less than 50-55 nt upstream from the next exon-exon junction greatly reduces the efficiency of NMD. If the PTC is close to the exon-exon junction, the ribosome removes the EJC thereby preventing the NMD machinery from binding and allowing translation of a truncated protein (da Costa et al., 2017; Hir et al., 2015). This is unlikely to be the reason for the increased stability of the mutant medium transcript in this report. The *Pnkd*c.415C>T mutation is 50 nt upstream from the next exon-exon junction in both of the medium and long transcripts. Given that only the medium transcript appears to avoid degradation, the proximity of the PTC to the next exon-exon junction is unlikely to be the mechanism of reduction of NMD efficiency.

Other less common mechanisms of NMD evasion are present in mammalian cells. For instance, PTC that are near the start of a transcript (<200 nt) have less efficient NMD. When the PTC is found in the first 100 nt of a transcript, NMD is rarely triggered regardless of the distance between the PTC and the next exon-exon junction

(Hir et al., 2015). Pnkd -medium and -long isoforms have different transcription start sites (Figure 2). The Pnkd-medium isoforms starts at the fourth exon while the long isoform begins at exon 1. The PTC resulting from the *Pnkd*c.415C>T mutation is 115 nt from the transcription start site of the medium transcript and 139 nt from the transcription start site of the long transcript. It's possible that the increase in distance of the PTC from the transcription start site in the long isoform accounts for its higher efficiency of degradation in comparison to the medium transcript.

While we have not yet shown that the mutant medium transcript is translated into a truncated protein, the stability of the mutant medium transcript indicates that a truncated protein may be present in both heterozygous and homozygous *Pnkd*c.415C>T mice. This truncated protein could potentially interfere with function of the wild-type Pnkd protein. The Pnkd long isoform has been shown to self-oligomerize somewhere between amino acids 132-166 (these residues correspond to amino acids 108-142 in the medium isoform) (Shen et al., 2011). The *Pnkd*c.415C>T SNV results in the replacement of a glutamine codon with a PTC at codon 139 in the long isoform and a PTC at codon 115 in the medium isoform. It is as yet undetermined if the medium isoform self-oligomerizes at these residues or if it undergoes multimerization at any other residues. However, it's possible that the mutant medium isoform may not be able to undergo multimerization due to exclusion of codons 115 onwards, and may be dysfunctional.

Mutations in mitochondrial expressed proteins are implicated in numerous neurological disorders including TD. Recurrent disruptions in the mitochondrial protease, IMMP2L, have been discovered in patients with TD. In a 2014 study, in higher incidence of deletions within the IMMP2L were found in individuals effected

with TD (3.7% compared to 0.9%). This gene has also been implicated in autism adding further support to a shared etiology neurodevelopmental disorders. The medium isoform is found in all cell types and localizes to the mitochondria where its function is unknown. Therefore, it remains possible that a dysfunctional truncated medium isoform causes or is a factor in the etiology of TD in the extended pedigree reported here. Previously, we hypothesized that haploinsufficiency of the long, neuronal, for of PNKD caused TD within the extended pedigree presented here (Figure 1, Sun et al., 2017). However, the qPCR data presented here warrants further investigation of a potential role for the medium isoform in both TD and brain function in general.

REFERENCES

Adam, D., 2013. On the spectrum. Nature 496, 6–8.

Avale, M.E., Falzone, T.L., Gelman, D.M., Low, M.J., Grandy, D.K., Rubinstein, M., 2004. The dopamine D4 receptor is essential for hyperactivity and impaired behavioral inhibition in a mouse model of attention deficit/hyperactivity disorder. Mol. Psychiatry 9, 718–726. doi:10.1038/sj.mp.4001474

Bailey KR, JN, C., 2009. Anxiety-Related Behaviors in Mice - PubMed - NCBI. Methods Behav. Anal. Neurosci. 21–26.

Bronfeld, M., Israelashvili, M., Bar-Gad, I., 2013. Pharmacological animal models of Tourette syndrome. Neurosci. Biobehav. Rev. 37, 1101–19. doi:10.1016/j.neubiorev.2012.09.010

Castellan Baldan, L., Williams, K.A., Gallezot, J.-D., Pogorelov, V., Rapanelli, M., Crowley, M., Anderson, G.M., Loring, E., Gorczyca, R., Billingslea, E., Wasylink,

S., Panza, K.E., Ercan-Sencicek, A.G., Krusong, K., Leventhal, B.L., Ohtsu, H., Bloch, M.H., Hughes, Z.A., Krystal, J.H., Mayes, L., de Araujo, I., Ding, Y.-S., State, M.W., Pittenger, C., 2014. Histidine decarboxylase deficiency causes tourette syndrome: parallel findings in humans and mice. Neuron 81, 77–90. doi:10.1016/j.neuron.2013.10.052

Cauchi, R and Tarnok, Z., 2012. GENETIC ANIMAL MODELS OF TOURETTE SYNDROME : THE LONG AND WINDING ROAD. Transl. Neurosci. 3, 153–159.

Chen, C.H., Fremont, R., Arteaga-bracho, E.E., 2015. NIH Public Access. Nat Neurosci 17, 1767–1775. doi:10.1038/nn.3868.Short

Cosgrove, V.E., Kelsoe, J.R., Suppes, T., 2016a. Toward a Valid Animal Model of Bipolar Disorder: How the Research Domain Criteria Help Bridge the Clinical-Basic Science Divide. Biol. Psychiatry 79, 62–70. doi:10.1016/j.biopsych.2015.09.002

Cosgrove, V.E., Kelsoe, J.R., Suppes, T., 2016b. Toward a Valid Animal Model of Bipolar Disorder: How the Research Domain Criteria Help Bridge the Clinical-Basic Science Divide. Biol. Psychiatry 79, 62–70. doi:10.1016/j.biopsych.2015.09.002

da Costa, P.J., Menezes, J., Romão, L., 2017. The role of alternative splicing coupled to nonsense-mediated mRNA decay in human disease. Int. J. Biochem. Cell Biol. 91, 168–175. doi:10.1016/j.biocel.2017.07.013

Dabrowski, M., Bukowy-Bieryllo, Z., Zietkiewicz, E., 2015. Translational readthrough potential of natural termination codons in eucaryotes – The impact of RNA

sequence. RNA Biol. 12, 950–958. doi:10.1080/15476286.2015.1068497

Deacon, R.M.J., 2006. Digging and marble burying in mice: simple methods for in vivo identification of biological impacts. Nat. Protoc. 1, 122–124. doi:10.1038/nprot.2006.20

Denys, D., de Vries, F., Cath, D., Figee, M., Vulink, N., Veltman, D.J., van der Doef, T.F., Boellaard, R., Westenberg, H., van Balkom, A., Lammertsma, A.A., van Berckel, B.N.M., 2013. Dopaminergic activity in Tourette syndrome and obsessive-compulsive disorder. Eur. Neuropsychopharmacol. 23, 1423–1431. doi:10.1016/j.euroneuro.2013.05.012

Dere, E., De Souza-Silva, M.A., Spieler, R.E., Lin, J.S., Ohtsu, H., Haas, H.L., Huston, J.P., 2004. Changes in motoric, exploratory and emotional behaviours and neuronal acetylcholine content and 5-HT turnover in histidine decarboxylase-KO mice. Eur. J. Neurosci. 20, 1051–1058. doi:10.1111/j.1460-9568.2004.03546.x

Eapen, V., 2015. Are there distinct subtypes in Tourette syndrome ? Pure-Tourette syndrome versus Tourette syndrome-plus , and simple versus complex tics 1431–1436.

Eichele, H., Plessen, K.J., 2013. Neural plasticity in functional and anatomical MRI studies of children with Tourette syndrome. Behav. Neurol. 27, 33–45. doi:10.3233/BEN-120294

Ercan-Sencicek, A.G., Stillman, A.A., Ghosh, A.K., Bilguvar, K., O'Roak, B.J., Mason, C.E., Abbott, T., Gupta, A., King, R.A., Pauls, D.L., Tischfield, J.A., Heiman, G.A., Singer, H.S., Gilbert, D.L., Hoekstra, P.J., Morgan, T.M., Loring, E., Yasuno, K., Fernandez, T., Sanders, S., Louvi, A., Cho, J.H., Mane, S., Colangelo,

C.M., Biederer, T., Lifton, R.P., Gunel, M., State, M.W., 2010. L-histidine decarboxylase and Tourette's syndrome. N. Engl. J. Med. 362, 1901–8. doi:10.1056/NEJMoa0907006

Felling, R.J., Singer, H.S., 2011. Neurobiology of tourette syndrome: current status and need for further investigation. J. Neurosci. 31, 12387–12395. doi:10.1523/JNEUROSCI.0150-11.2011

Fernandez, T. V., Sanders, S.J., Yurkiewicz, I.R., Ercan-Sencicek, A.G., Kim, Y.-S., Fishman, D.O., Raubeson, M.J., Song, Y., Yasuno, K., Ho, W.S.C., Bilguvar, K., Glessner, J., Chu, S.H., Leckman, J.F., King, R.A., Gilbert, D.L., Heiman, G.A., Tischfield, J.A., Hoekstra, P.J., Devlin, B., Hakonarson, H., Mane, S.M., Günel, M., State, M.W., 2012. Rare Copy Number Variants in Tourette Syndrome Disrupt Genes in Histaminergic Pathways and Overlap with Autism. Biol. Psychiatry 71, 392–402. doi:10.1016/j.biopsych.2011.09.034

Ganos, C., 2016. Tics and Tourette's: update on pathophysiology and tic control. Curr. Opin. Neurol. 29.

Gardiner, A.R., Jaffer, F., Dale, R.C., Labrum, R., Erro, R., Meyer, E., Xiromerisiou, G., Stamelou, M., Walker, M., Kullmann, D., Warner, T., Jarman, P., Hanna, M., Kurian, M.A., Bhatia, K.P., Houlden, H., 2015. The clinical and genetic heterogeneity of paroxysmal dyskinesias. doi:10.1093/brain/awv310

Glerup, S., Olsen, D., Vaegter, C.B., Gustafsen, C., Sjoegaard, S.S., Hermey, G., Kjolby, M., Molgaard, S., Ulrichsen, M., Boggild, S., Skeldal, S., Fjorback, A.N., Nyengaard, J.R., Jacobsen, J., Bender, D., Bjarkam, C.R., Sørensen, E.S., Füchtbauer, E.M., Eichele, G., Madsen, P., Willnow, T.E., Petersen, C.M.,

Nykjaer, A., 2014. SorCS2 regulates dopaminergic wiring and is processed into an apoptotic two-chain receptor in peripheral glia. Neuron 82, 1074–1087. doi:10.1016/j.neuron.2014.04.022

Godar, S.C., Mosher, L.J., Di Giovanni, G., Bortolato, M., 2014. Animal models of tic disorders: a translational perspective. J. Neurosci. Methods 238, 54–69. doi:10.1016/j.jneumeth.2014.09.008

Goetz, C.G., Chmura, T.A., Lanska, D.J., 2001. History of Tic Disorders and Gilles de la Tourette Syndrome : Part 5 of the MDS-Sponsored History of Movement Disorders 16, 346–349.

Gong, Y., He, H., Liu, H., Zhang, C., Zhao, W., Shao, R.G., 2014. Phosphorylation of myofibrillogenesis regulator-1 activates the MAPK signaling pathway and induces proliferation and migration in human breast cancer MCF7 cells. FEBS Lett. 588, 2903–2910. doi:10.1016/j.febslet.2014.07.018

Hir, H. Le, Saulière, J., Wang, Z., 2015. The exon junction complex as a node of post-transcriptional networks. Nat. Rev. Mol. Cell Biol. 17, 41–54. doi:10.1038/nrm.2015.7

Hirschtritt, M.E., Lee, P.C., Pauls, D.L., Dion, Y., Grados, M.A., Illmann, C., King, R.A., Sandor, P., Mcmahon, W.M., Lyon, G.J., Cath, D.C., Kurlan, R., Robertson, M.M., Med, D., Osiecki, L., Scharf, J.M., 2016. Lifetime Prevalence, Age of Risk, and Genetic Relationships of Comorbid Psychiatric Disorders in Tourette Syndrome 94143, 325–333. doi:10.1001/jamapsychiatry.2014.2650

Hu, H., Roach, J.C., Coon, H., Guthery, S.L., Voelkerding, K. V, Margraf, R.L., Durtschi, J.D., Tavtigian, S. V, Shankaracharya, Wu, W., Scheet, P., Wang, S.,

Xing, J., Glusman, G., Hubley, R., Li, H., Garg, V., Moore, B., Hood, L., Galas, D.J., Srivastava, D., Reese, M.G., Jorde, L.B., Yandell, M., Huff, C.D., 2014. A unified test of linkage analysis and rare-variant association for analysis of pedigree sequence data. Nat. Biotechnol. 32, 663–669. doi:10.1038/nbt.2895

Huisman-van Dijk, H.M., Schoot, R. van de, Rijkeboer, M.M., Mathews, C.A., Cath, D.C., 2016a. The relationship between tics, OC, ADHD and autism symptoms: A cross- disorder symptom analysis in Gilles de la Tourette syndrome patients and family-members. Psychiatry Res. 1–9. doi:10.1016/j.psychres.2016.01.051

Huisman-van Dijk, H.M., Schoot, R. van de, Rijkeboer, M.M., Mathews, C.A., Cath, D.C., 2016b. The relationship between tics, OC, ADHD and autism symptoms: A cross- disorder symptom analysis in Gilles de la Tourette syndrome patients and family-members. Psychiatry Res. 237, 138–146. doi:10.1016/j.psychres.2016.01.051

Insel, T., Cuthbert, B., Garvey, M., Heinssen, R., Pine, D.S., Quinn, K., Sanislow, C., Wang, P., 2010. Research Domain Criteria (RDoC): Toward a new classification framework for research on mental disorders. Am. J. Psychiatry 167, 748–751. doi:10.1176/appi.ajp.2010.09091379

Javitt, D.C., Freedman, R., 2015. Sensory processing dysfunction in the personal experience and neuronal machinery of schizophrenia. Am. J. Psychiatry 172, 17–31. doi:10.1176/appi.ajp.2014.13121691

Kalanithi, P.S.A., Zheng, W., Kataoka, Y., DiFiglia, M., Grantz, H., Saper, C.B., Schwartz, M.L., Leckman, J.F., Vaccarino, F.M., 2005. Altered parvalbumin-positive neuron distribution in basal ganglia of individuals with Tourette

syndrome. Proc. Natl. Acad. Sci. U. S. A. 102, 13307–12. doi:10.1073/pnas.0502624102

Kozak, M.J., Cuthbert, B.N., 2016. The NIMH Research Domain Criteria Initiative: Background, Issues, and Pragmatics. Psychophysiology 53, 286–297. doi:10.1111/psyp.12518

Leckman, J.F., Bloch, M.H., Smith, M.E., Larabi, D., Hampson, M., 2010. Neurobiological substrates of Tourette's disorder. J. Child Adolesc. Psychopharmacol. 20, 237–47. doi:10.1089/cap.2009.0118

Leckman, J.F., Zhang, H., Vitale, A., Lahnin, F., Lynch, K., Bondi, C., Kim, Y.-S., Peterson, B.S., 1998. Course of Tic Severity in Tourette Syndrome: The First Two Decades. Pediatrics 102, 14–19.

Lee, H.Y., Nakayama, J., Xu, Y., Fan, X., Karouani, M., Shen, Y., Pothos, E.N., Hess, E.J., Fu, Y.H., Edwards, R.H., Ptaćek, L.J., 2012. Dopamine dysregulation in a mouse model of paroxysmal nonkinesigenic dyskinesia. J. Clin. Invest. 122, 507–518. doi:10.1172/JCI58470

Lee, H.Y., Xu, Y., Huang, Y., Ahn, A.H., Auburger, G.W.J., Pandolfo, M., Kwieci??ski, H., Grimes, D.A., Lang, A.E., Nielsen, J.E., Averyanov, Y., Servidei, S., Friedman, A., Van Bogaert, P., Abramowicz, M.J., Bruno, M.K., Sorensen, B.F., Tang, L., Fu, Y.H., Pt????ek, L.J., 2004. The gene for paroxysmal non-kinesigenic dyskinesia encodes an enzyme in a stress response pathway. Hum. Mol. Genet. 13, 3161–3170. doi:10.1093/hmg/ddh330

Lindeboom, R.G.H., Supek, F., Lehner, B., 2016. The rules and impact of nonsense-mediated mRNA decay in human cancers. Nat. Genet. 48, 1112–1118.

doi:10.1038/ng.3664

Liu, H.-X., Cartegni, L., Zhang, M.Q., Krainer, A.R., 2001. A mechanism for exon skipping caused by nonsense or missense mutations in BRCA1 and other genes. Nat. Genet. 27, 55.

Lutter, M., Croghan, A.E., Cui, H., 2016. Escaping the Golden Cage: Animal Models of Eating Disorders in the Post-Diagnostic and Statistical Manual Era. Biol. Psychiatry 79, 17–24. doi:10.1016/j.biopsych.2015.02.006

Macrì, S., Onori, M.P., Roessner, V., Laviola, G., 2013. Animal Models Recapitulating the Multifactorial Origin of Tourette Syndrome, 1st ed, Advances in the Neurochemistry and Neuropharmacology of Tourette Syndrome. Elsevier Inc. doi:10.1016/B978-0-12-411546-0.00008-1

Moya, P.R., Wendland, J.R., Rubenstein, L.M., Timpano, K.R., Heiman, G.A., Tischfield, J.A., King, R.A., Andrews, A.M., Ramamoorthy, S., Mcmahon, F.J., Murphy, D.L., 2013. Common and rare alleles of the serotonin transporter gene, SLC6A4, associated with Tourette's disorder. Mov. Disord. 28, 1263–1270. doi:10.1002/mds.25460

Müller-Vahl, K.R., Kaufmann, J., Grosskreutz, J., Dengler, R., Emrich, H.M., Peschel, T., 2009. Prefrontal and anterior cingulate cortex abnormalities in Tourette Syndrome: evidence from voxel-based morphometry and magnetization transfer imaging. BMC Neurosci. 10, 47. doi:10.1186/1471-2202-10-47

Obeso, J.A., Rodriguez-Oroz, M.C., Stamelou, M., Bhatia, K.P., Burn, D.J., 2014. The expanding universe of disorders of the basal ganglia. Lancet (London, England) 384, 523–31. doi:10.1016/S0140-6736(13)62418-6

Paschou, P., 2013. Neuroscience and Biobehavioral Reviews The genetic basis of Gilles de la Tourette Syndrome. Neurosci. Biobehav. Rev. 37, 1026–1039. doi:10.1016/j.neubiorev.2013.01.016

Patrick, C.J., Hajcak, G., 2016. RDoC: Translating promise into progress. Psychophysiology 53, 415–424. doi:10.1111/psyp.12612

Prasun, P., Pradhan, M., Agarwal, S., 2007. One gene, many phenotypes. J. Postgrad. Med. 53, 257–61. doi:10.4103/0022-3859.33968

Sarnyai, Z., Alsaif, M., Bahn, S., Ernst, A., Guest, P.C., Hradetzky, E., Kluge, W., Stelzhammer, V., Wesseling, H., 2011. Behavioral and Molecular Biomarkers in Translational Animal Models for Neuropsychiatric Disorders, International Review of Neurobiology. doi:10.1016/B978-0-12-387718-5.00008-0

Shen, Y., Ge, W.-P., Li, Y., Hirano, A., Lee, H.-Y., Rohlmann, A., Missler, M., Tsien, R.W., Jan, L.Y., Fu, Y.-H., Ptáček, L.J., 2015. Protein mutated in paroxysmal dyskinesia interacts with the active zone protein RIM and suppresses synaptic vesicle exocytosis. Proc. Natl. Acad. Sci. U. S. A. 112, 2935–41. doi:10.1073/pnas.1501364112

Shen, Y., Lee, H.Y., Rawson, J., Ojha, S., Babbitt, P., Fu, Y.H., Ptácek, L.J., 2011. Mutations in PNKD causing paroxysmal dyskinesia alters protein cleavage and stability. Hum. Mol. Genet. 20, 2322–2332. doi:10.1093/hmg/ddr125

Smoller, J., Kendler, K., Craddock, N., 2013. Identification of risk loci with shared effects on five major psychiatric disorders: a genome-wide analysis. Lancet 381, 1371–9. doi:10.1016/S0140-6736(12)62129-1

Steimer, T., Driscoll, P., 2003. Divergent Stress Responses and Coping Styles in

Psychogenetically Selected Roman High-(RHA) and Low-(RLA) Avoidance Rats: Behavioural, Neuroendocrine and Developmental Aspects. Stress 6, 87–100. doi:10.1080/1025389031000111320

Sun, N., Nasello, C., Deng, L., Wang, N., Zhang, Y., Xu, Z., Song, Z., Kwan, K., King, R.A., Pang, Z.P., Xing, J., Heiman, G.A., 2017. The PNKD gene is associated with Tourette Disorder or Tic disorder in a multiplex family. Mol. Psychiatry 1–9. doi:10.1038/mp.2017.179

Swerdlow, N.R., 2013. Neuroscience and Biobehavioral Reviews Update : Studies of prepulse inhibition of startle , with particular relevance to the pathophysiology or treatment of Tourette Syndrome. Neurosci. Biobehav. Rev. 37, 1150–1156. doi:10.1016/j.neubiorev.2012.09.002

Tao, T.Q., Wang, X.R., Liu, M., Xu, F.F., Liu, X.H., 2015. Myofibrillogenesis regulator-1 attenuated hypoxia/reoxygenation-induced apoptosis by inhibiting the PERK/Nrf2 pathway in neonatal rat cardiomyocytes. Apoptosis 20, 285–297. doi:10.1007/s10495-014-1081-1

Thomas, A., Burant, A., Bui, N., Graham, D., Yuva-Paylor, L.A., Paylor, R., 2009. Marble burying reflects a repetitive and perseverative behavior more than novelty-induced anxiety. Psychopharmacology (Berl). 204, 361–373. doi:10.1007/s00213-009-1466-y

Tobe, R.H., Bansal, R., Xu, D., Hao, X., Liu, J., Sanchez, J., Peterson, B.S., 2010. Cerebellar morphology in tourette syndrome and obsessive-compulsive disorder. Ann. Neurol. 67, 479–487. doi:10.1002/ana.21918

Warr, A., Robert, C., Hume, D., Archibald, A., Deeb, N., Watson, M., 2015. Exome

Sequencing: Current and Future Perspectives. G3 (Bethesda). 5, g3.115.018564-. doi:10.1534/g3.115.018564

Xu, M., Kobets, A., Du, J.-C., Lennington, J., Li, L., Banasr, M., Duman, R.S., Vaccarino, F.M., DiLeone, R.J., Pittenger, C., 2015. Targeted ablation of cholinergic interneurons in the dorsolateral striatum produces behavioral manifestations of Tourette syndrome. Proc. Natl. Acad. Sci. U. S. A. 112, 893–8. doi:10.1073/pnas.1419533112

Yu, D., Mathews, C.A., Scharf, J.M., Neale, B.M., Davis, L.K., Gamazon, E.R., Derks, E.M., Evans, P., Edlund, C.K., Crane, J., Fagerness, J.A., Osiecki, L., Gerber, G., Haddad, S., Illmann, C., McGrath, L.M., Mayerfeld, C., Arepalli, S., Barlassina, C., Barr, C.L., Bellodi, L., Benarroch, F., Bedoya Berrió, G., Bienvenu, J., Black, D.W., Bloch, M.H., Brentani, H., Bruun, R.D., Budman, C.L., Camarena, B., Campbell, D.D., Cappi, C., Cardona Silgado, J.C., Cavallini, M.C., Chavira, D.A., Chouinard, S., Cook, E.H., Cookson, M.R., Coric, V., Cullen, B., Cusi, D., Delorme, R., Denys, D., Dion, Y., Eapen, V., Egberts, K., Falkai, P., Fernandez, T., Fournier, E., Garrido, H., Geller, D., Gilbert, D.L., Girard, S.L., Grabe, H.J., Grados, M.A., Greenberg, B.D., Gross-Tsur, V., Grünblatt, E., Hardy, J., Heiman, G.A., Hemmings, S.M.J., Herrera, L.D., Hezel, D.M., Hoekstra, P.J., Jankovic, J., Kennedy, J.L., King, R.A., Konkashbaev, A.I., Kremeyer, B., Kurlan, R., Lanzagorta, N., Leboyer, M., Leckman, J.F., Lennertz, L., Liu, C., Lochner, C., Lowe, T.L., Lupoli, S., Macciardi, F., Maier, W., Manunta, P., Marconi, M., McCracken, J.T., Mesa Restrepo, S.C., Moessner, R., Moorjani, P., Morgan, J., Muller, H., Murphy, D.L., Naarden, A.L., Nurmi, E., Cornejo Ochoa, W., Ophoff,

R.A., Pakstis, A.J., Pato, M.T., Pato, C.N., Piacentini, J., Pittenger, C., Pollak, Y., 2015. Cross-disorder genome-wide analyses suggest a complex genetic relationship between tourette's syndrome and OCD. Am. J. Psychiatry 172, 82–93. doi:10.1176/appi.ajp.2014.13101306

Yu, T.W., Chahrour, M.H., Coulter, M.E., Jiralerspong, S., Ataman, B., Harmin, D. a, Adli, M., Malik, a N., Gama, D., Lim, E.T., Sanders, S.J., Mochida, G.H., Partlow, J.N., Sunu, C.M., Felie, J.M., Rodriguez, J., Nasir, R.H., Ware, J., Joseph, R.M., Hill, R.S., Kwan, B.Y., Mukaddes, N.M., Hashmi, a, Balkhy, S., 2013. NIH Public Access autism 77, 259–273. doi:10.1016/j.neuron.2012.11.002.Using

Zetoune, A.B., Fontanière, S., Magnin, D., Anczuków, O., Buisson, M., Zhang, C.X., Mazoyer, S., 2008. Comparison of nonsense-mediated mRNA decay efficiency in various murine tissues. BMC Genet. 9, 83. doi:10.1186/1471-2156-9-83

Zimmermann, A.M., Jene, T., Wolf, M., Görlich, A., Gurniak, C.B., Sassoè-Pognetto, M., Witke, W., Friauf, E., Rust, M.B., 2015. Attention-Deficit/Hyperactivity Disorder-like Phenotype in a Mouse Model with Impaired Actin Dynamics. Biol. Psychiatry 78, 95–106. doi:10.1016/j.biopsych.2014.03.011